12. ANALOGUES TO SATURATED ZONE TRANSPORT

12.1 INTRODUCTION

This section discusses analogues to transport in a saturated environment under oxidizing conditions, such as that at Yucca Mountain. Most of the analogue sites studied to date in saturated environments occur in rock types dissimilar to the saturated zone (SZ) at Yucca Mountain, e.g., fractured crystalline granite or gneiss, or sandstone. However, some aspects of these systems have attributes or demonstrate processes that warrant attention with respect to Yucca Mountain and are included in this section. Section 12.1 briefly summarizes the main conclusions of past Yucca Mountain Site Characterization Project (YMP) analogue studies with respect to SZ transport. Section 12.2 provides a background by describing the SZ flow system at Yucca Mountain. Section 12.3 is a study of transport plumes formed from uranium mill tailings at selected sites in the western United States, and the relevance of this information to saturated transport in alluvium at Yucca Mountain. Section 12.4 provides examples from analogues of matrix diffusion and colloid transport in the SZ. The main ideas and conclusions are presented in Section 12.5.

12.1.1 Insights into SZ Transport from Previous Analogue Studies

Some of the processes relevant to radionuclide transport at saturated sites were discussed in *Yucca Mountain Site Description* (CRWMS M&O 2000 [151945], Section 13.4.3). The main points of those discussions are summarized here.

- Filtration of particulate matter is an efficient process at Poços de Caldas (CRWMS M&O 2000 [151945], Section 13.4.3.3). The colloidal material acts as largely irreversible sinks for many immobile elements, such as thorium and rare-earth elements.

- The redox front at Poços de Caldas provided direct evidence of the operation of flow channeling in fractures and solute transport in the rock matrix as the key controls on the shape and movement of the redox front. The very slow, diffusion-dominated movement of the redox front plays a significant role in retarding many trace elements (CRWMS M&O 2000 [151945], Section 13.4.3.3; Romero et al. 1992 [157573], pp. 471–472).

- Poços de Caldas also highlighted the importance of amorphous phases in suspension or as coatings on rock as the principal sorptive surfaces for many trace elements in solution (CRWMS M&O 2000 [151945], Section 13.4.3.3). Some of the fixing processes appeared to be irreversible over long time scales, compared to reversible sorption used in Performance Assessment (PA) models. Sorption onto fracture coatings, particularly calcite, also efficiently retards uranium transport in fractures at Palmottu (CRWMS M&O 2000) [151945], Section 13.4.3.3).

- The Chernobyl study (CRWMS M&O 2000 [151945], Section 13.4.3.3) showed that pathways of rapid groundwater contamination around Chernobyl may not be directly connected to the pathways of near-surface zones of preferential flow.

Other analogues were mentioned as multiple lines of evidence in *FY 01 Supplemental Science and Performance Analyses, Volume 1: Scientific Bases and Analyses* (BSC 2001 [155950], Section 12.4). Using Yucca Mountain as a self-analogue, it was possible to interpret groundwater hydrochemical data to estimate flow paths in the vicinity of Yucca Mountain (BSC 2001 [155950], Section 12.4.1). These estimated flow paths were shown to be consistent with flow paths predicted by the site-scale SZ flow model.

The initial phase of investigation of the Uranium Mill Tailing Remedial Action (UMTRA) sites discovered that some fraction of the total inventory of uranium mill tailings appears to be transported as a nonsorbing to weakly sorbing species under oxidizing conditions (BSC 2001 [155950], Section 12.4.2). This supported the TSPA-SR treatment of uranium as weakly sorbing (BSC 2001 [155950], Section 12.4.2).

12.2 HYDROGEOLOGY AND FRACTURE MINERALOGY OF THE SATURATED ZONE

The water table near the proposed Yucca Mountain repository block is currently at an elevation of approximately 730 m, more than 300 m below the proposed repository horizon (DOE 1998 [100548], Section 2.2.4). Water infiltrating the unsaturated zone (UZ) becomes recharge to the regional flow system. Water moves generally southeast beneath the (UZ) site before flowing south out of the volcanic rocks and into the thick valley fill of the Amargosa Valley. The hydraulic gradient is very low (~0.0001; Fridrich et al. 1994 [100575], p. 138) downgradient from Yucca Mountain, so that travel time of groundwater may be long. Near Yucca Mountain, volcanic rocks up to several thousand meters thick overlie the Paleozoic and older rocks of the region (DOE 1998 [100548], Section 2.2.4.1). Their hydrologic properties change substantially over short distances, which produces a complex hydrogeology. The volcanic-rock section becomes thinner to the south and is a lesser component of the saturated zone flow system in southern Amargosa Valley, where the major aquifer consists of Quaternary-Tertiary heterogeneous valley-fill deposits.

The dominant regional aquifer is the Paleozoic carbonate aquifer, consisting of marine limestones, dolomites, and minor clastic sediments thousands of meters thick. In the vicinity of Yucca Mountain, the carbonate aquifer is not tapped as a source of groundwater because of its great depth (DOE 1998 [100548], Section 2.2.4.1).

Luckey et al. (1996 [100465], pp. 18–20) divided the volcanic rocks below the water table into four hydrogeologic units. From top to bottom, these are the upper volcanic aquifer, the upper volcanic confining unit, the lower volcanic aquifer, and the lower volcanic confining unit. The upper volcanic aquifer is composed of the Topopah Spring Tuff, which occurs in the UZ near the repository, but is present beneath the water table to the east and south of the potential repository and in Crater Flat. The upper volcanic confining unit includes the Calico Hills Formation and the uppermost, unfractured part of the Prow Pass Tuff in areas where they are saturated. The lower volcanic aquifer includes most of the Crater Flat Group (Luckey et al. 1996 [100465] pp. 18–20), and the lower volcanic confining unit includes the lowermost Crater Flat Group and deeper tuffs, lavas, and flow breccias. The upper volcanic aquifer underlying Yucca Mountain is generally productive and provides groundwater for the site. The main distinction between SZ volcanic aquifers and confining units is that the aquifers tend to be more welded and contain more

permeable fractures than the aquitards. However, alteration of the nonwelded tuffs to zeolites and clays, which reduces permeability, is more pronounced at depth. The increase of pressure with depth also reduces fracture permeability, such that the overall tendency is toward decreased permeability with depth, even in aquifers.

The chemistry of SZ waters beneath Yucca Mountain (Oliver and Root 1997 [100069]) reflects processes that affected these waters as they flowed to the Yucca Mountain area from recharge areas to the north (McKinley et al. 1991 [116222]). In general, they are dilute sodium bicarbonate waters that are neutral to mildly alkaline and mildly oxidizing. Similarities between the composition of SZ waters in the recharge areas north of Yucca Mountain and those beneath Yucca Mountain suggest that water compositions primarily reflect water-rock interactions in the recharge areas (DOE 1998 [100548], Section 2.2.4.3).

After reaching the water table, flow continues generally to the southeast away from the potential repository. The majority of saturated flow occurs in zones with enhanced permeabilities caused by fractures. Retardation processes such as sorption, matrix diffusion, and dispersion would also function in the SZ. Water may contact sorbing zeolites in the Calico Hills Formation and Prow Pass Tuff, and, as in the UZ, fracture minerals may have a significant effect on both flow and transport.

Fracture-filling minerals in the SZ include smectite, manganese oxide minerals, hematite, quartz, opal-CT, calcite, and clinoptilolite and mordenite, the same zeolites that characterize the altered rock matrix below the water table (Carlos et al. 1995 [101326], pp. 8–12). Laboratory experiments have shown that fractures containing smectite, manganese oxides, and calcite have particular affinity for plutonium retention (DOE 1998 [100548], Section 2.2.5.2). Thus, analogues related to transport through saturated, oxidizing environments need to consider the role of fracture-filling minerals such as these in retarding the migration of radionuclides.

12.3 URANIUM MILL TAILINGS

12.3.1 Purpose and Approach

This section summarizes pertinent information on the transport of uranium and other constituents of interest in alluvial aquifers at UMTRA sites. The YMP is particularly interested in the dispersion characteristics of the contaminant plumes and in the retardation behavior of constituents, such as uranium, that are found in nuclear waste to be emplaced in a repository.

The scope of Section 12.3 is limited to a review of the subsurface transport behavior of uranium and other constituents of interest at UMTRA sites. All UMTRA sites have been evaluated to identify those sites appropriate for more detailed analysis. The emphasis here is on the transport behavior of uranium and other constituents in alluvial deposits. This is because the potential transport pathways from Yucca Mountain to the accessible environment pass through alluvium and because there are no UMTRA sites with bedrock similar to the volcanic rocks at Yucca Mountain.

The approach is to evaluate the UMTRA sites in terms of aquifer materials, hydrologic characteristics, and groundwater chemistry. Those sites that are closest in hydrologic and

chemical characteristics to the alluvium downgradient from Yucca Mountain and for which sufficient data are available for detailed transport analysis are considered in more detail.

12.3.2 Background

The UMTRA Project was authorized by Congress in 1978 to clean up 24 inactive uranium ore processing sites (DOE 1996 [154693]). Currently, there are 20 UMTRA Project sites in the continental United States, located mostly in the western states (Figure 12-1). Many of the sites are located in the Rocky Mountain states of Colorado (seven sites), Utah (three sites), Wyoming (two sites), New Mexico (two sites), and Idaho (one site). Sites are also located in Arizona (two sites), Oregon (one site), and Texas (one site) (DOE 2000 [157603]).

Most of the sites consisted of a uranium processing mill with associated waste streams and ore and tailings piles. The ore and tailings piles were situated directly on surface soils. Rain and snow melt percolated through the piles, leaching uranium and other constituents, before entering the underlying shallow groundwater systems. The UMTRA Project has monitored the concentrations of radionuclides and other contaminants in shallow groundwaters beneath and downgradient from these sites for 15 to 20 years. The information obtained provides useful insight on the fate and transport of uranium and related ore constituents in shallow aquifers. The information obtained on transport in alluvial aquifers could be particularly useful in the development of models and calculations for radionuclide transport in shallow alluvial aquifers down gradient from Yucca Mountain.

12.3.3 Selection of Analogue Sites

The magnitude of operations at the various UMTRA sites was quite variable. Sites such as Grand Junction, Rifle, and Naturita in Colorado had large operations that resulted in large tailings piles. Operations at Cannonsburg in Pennsylvania and Spook in Wyoming were much smaller, with correspondingly smaller tailings piles. Other sites were in between these two groups in terms of magnitude of operations and size of the tailings piles. The magnitude of the operation is important in this discussion, because the magnitude of the site-characterization activities undertaken by the UMTRA Project was generally proportional to the magnitude of the operation at a given site. To be useful to the Yucca Mountain Project, detailed site-characterization data are required on the flow and transport systems at these sites. Only a limited number of UMTRA sites have been investigated in sufficient detail to be of use as analogues to the transport of uranium and other constituents of interest in the alluvial part of the Yucca Mountain flow system.

The history of operations at the various sites was also quite variable. Operations at the Old Rifle site started as early as 1924. Most of the sites started operation in the mid to late 1950s and ended operations in the early 1960s to early 1970s. During the 1980s and 1990s, the tailings piles located at the 24 sites were either capped in place or removed to another location and encapsulated. Therefore, the tailings piles were sources of contaminants for subsurface transport for, at most, 30 to 70 years.

The ores processed at the various locations contained other chemical elements besides uranium and its daughter products. These elements included vanadium, arsenic, selenium, manganese, molybdenum, barium, and other trace metals. Most of these ore “byproducts” ended up in the

tailings piles. In addition, chemicals used in processing the ore were also dumped on the tailings piles. Important among the latter were sulfuric acid, nitric acid, ammonium hydroxide, and organic complexing agents. While the mills were in operation, rain and melted snow infiltrated into the uncovered tailings piles and leached constituents from the tailings. Liquid spills or leaks from site operations also infiltrated into the subsurface. These spill, leak, and leach solutions have since percolated downward through the subsoils and sediments beneath the sites and reached groundwater, forming plumes of contaminants in shallow aquifers.

Those UMTRA sites where the most extensive subsurface characterization and groundwater monitoring activities were performed are of the most interest to the YMP. The transport of contaminants in groundwater is controlled by numerous site-specific factors. Part of the value of UMTRA sites as analogues, therefore, is the site-specific information they can provide on the factors that control the transport behavior of important constituents such as uranium. Other parameters used to screen sites for more detailed discussion include the hydrogeology and hydrology of the shallow aquifers, and groundwater chemistry. The intent was to select sites with alluvial aquifers and low-ionic-strength groundwaters. The sites chosen for detailed discussion in this report are the Gunnison and New Rifle sites in Colorado.

12.3.3.1 Gunnison, Colorado, UMTRA Site

The following discussion is based primarily on information presented in the *Final Site Observational Work Plan for the UMTRA Project Gunnison Site* (DOE 2001 [156666]) and "Groundwater Hydrology Report" Attachment 3 of *Remedial Action Plan and Site Design for Stabilization of the Inactive Uranium Mill Tailings Site at Gunnison, Colorado, Final* (DOE 1992 [154692]). The Gunnison processing site is located adjacent to the city of Gunnison in Gunnison County, Colorado, on a drainage divide between the Gunnison River and Tomichi Creek in the Gunnison River valley (Figure 12-2). Uranium was processed at the site from 1958 to 1962. Approximately 719,000 yd^3 (550,000 m^3) of contaminated material including tailings were originally present on 68 acres (28 hectares). Between 1992 and 1995, the contaminated material was moved to the Gunnison disposal site, approximately 6 mi (10 km) from the processing site.

The processing site was located on floodplain alluvium between the Gunnison River and Tomichi Creek. The site is about 0.4 mi (0.6 km) east of the Gunnison River and 0.4 mi (0.6 km) west of Tomichi Creek (Figure 12-2). It is bounded on the west by small storm drainage ditches and on the south and west by irrigation ditches. The climate at the site is semi-arid, with an average annual precipitation of 10.5 in. (27 cm), of which approximately half is contributed by snowfall (DOE 2001 [156666], Section 3.1). The average depth to groundwater beneath the site is 5 ft (1.5 m). The uppermost (unconfined) aquifer at the site is in the floodplain alluvium of the Gunnison River and Tomichi Creek. These alluvial deposits extend to at least 110 ft (34 m) beneath the processing site. The aquifer is recharged from rain, snowmelt, the Gunnison River, Tomichi Creek, and seasonal irrigation ditches around the site. The groundwater flows southwest at an average velocity of 270 ft (82 m) per year. Groundwater from beneath the site discharges into the Gunnison River and Tomichi Creek (DOE 1992 [154692], pp. 18-20).

Tailings seepage has contaminated the alluvial groundwater beneath and downgradient from the processing site. Sulfuric acid was used extensively in ore processing at the site (DOE 1992

[154692], p. 23). Because sulfate is a conservative constituent (i.e., is not retarded) in oxidizing groundwaters, it can be used to delineate the maximum extent of movement of site-related contaminants in groundwater. A sulfate plume has been delineated that originates at the site and extends approximately 7,000 ft (2,000 m) in a southwesterly direction (Figure 12-3). Even though the plume intersects, and possibly flows beneath, the Gunnison River, sulfate is conservative relative to uranium at this site. The inferred areal shape of the plume suggests only limited lateral dispersion over most of the length of the plume. A lateral pinching of the plume is also inferred by its shape. Borehole lithology logs show a local variation in unit thicknesses close to the narrowing of the plume. Here, the uppermost sand and gravel unit is about twice its thickness in adjacent boreholes and appears to fill a paleochannel cut into the underlying clayey sand and gravel unit (DOE 1992 [154692], p. 16). The highest concentration contours of both the sulfate and uranium plumes (DOE 1992 [154692], pp. 31, 35, Figures 12-3, 12-4) are tied to a water analysis from this location. Therefore, the widths of the plumes may be locally constrained by geohydrologic variations in the subsurface alluvial deposits. Interpretations of plume shape must be tempered by the fact that the number of sampling points available to construct the plume map was limited. The maximum concentrations of sulfate in groundwaters along the length of the plume show only limited variation (715–378 mg/L). This suggests that downgradient dilution of contaminants originating at the processing site is limited.

A uranium plume has also been delineated in association with the Gunnison site (Figure 12-4). The inferred plume has a shape and lateral extent very similar to the inferred sulfate plume (Figure 12-3). The similar shapes of the two inferred plume maps suggest that the narrow shape of the uranium plume is locally controlled by geohydrologic variations in the alluvium, described above, and not directly related to chemical conditions in the alluvial aquifer. For example, the possibility that lower uranium concentrations outside the inferred plume could simply reflect more reducing conditions that lead to the removal of uranium from groundwater is not supported by the data. The similarity in the lengths of the inferred uranium and sulfate plumes suggests that at least some of the uranium originating from the site may have been transported with little or no retardation. However, the groundwater concentrations of uranium decrease more rapidly with distance from the site than the sulfate concentrations. One possible explanation for the different concentration gradients is that the source terms increased with time. Another possible explanation is that the travel time for uranium was longer than the travel time for sulfate (i.e., that uranium was retarded to some degree). Laboratory data on sorption coefficients for uranium on alluvium from this area support the latter interpretation. The sorption coefficient values obtained for two alluvium samples were 1.70 and 5.24 mL/g (DOE 2000 [156666], Table 4-7). Note that dilution alone is not a likely explanation for the decreasing uranium concentrations downgradient, because sulfate concentrations do not decrease proportionately downgradient.

In summary, the groundwater data for the Gunnison site yield several conclusions that may be significant with regard to radionuclide transport in alluvium at the Yucca Mountain site. To the extent that the hydrology of the alluvial aquifers at the Gunnison site and Yucca Mountain are comparable, the Gunnison data suggest that: (1) lateral dispersion may be very limited downgradient, (2) dilution may not be a significant process over the transport distance in alluvium, and (3) uranium may be only slightly retarded by interaction with aquifer materials.

12.3.3.2 New Rifle Site, Rifle, Colorado

The Rifle UMTRA site is located along the Colorado River approximately 90 miles (144 km) east of Grand Junction, Colorado. The Rifle site actually consists of two separate sites, known as "Old Rifle" and "New Rifle." The Old Rifle site is located approximately 2.3 mi (3.7 km) northeast of the New Rifle site (Figure 12-5). The New Rifle site has been studied in greater detail and is for this reason the subject of this summary. The discussion in this section is based primarily on the *Final Site Observational Work Plan for the UMTRA Project New Rifle Site, Volumes 1 and 2* (DOE 1999 [154687]).

The New Rifle site processed uranium and vanadium ores from 1958 to 1984. The site is located within the broad alluvial floodplain of the Colorado River (Figure 12-6). The New Rifle site occupied much of the width of the Colorado River floodplain in a north-south direction (approximately 3,000 ft) (500 m), with the river located on the southern portion of the floodplain. The ore storage areas were located in the easternmost (upgradient) portion of the site, whereas the tailings pile was located in the western portion of the site. The mill and other buildings were located between the tailings pile and the ore storage areas. Approximately 3.5 million yd^3 (2.7 million m^3) of contaminated material were present on 238 acres (96 hectares) at the site. The transfer of this contaminated material to a disposal cell was completed in 1996.

The climate in the Rifle region is semi-arid, with an average total annual precipitation of 11 in. (28 cm) of which approximately one third is contributed by snowfall (DOE 1999 [154687], Section 3.2). The New Rifle site is underlain by 20–30 ft (6–9 m) of alluvium deposited by the Colorado River (DOE 1999 [154687], Section 5.1.2.2). Unconfined groundwater is present at the base of the alluvium at a depth of 5–10 ft (1.5–3 m) below the ground surface. In general, groundwater flows west-southwest in the alluvium and in the underlying bedrock (DOE 1999 [154687], Section 5.2.2). The alluvial deposits north of the river pinch out approximately 4 mi (6.4 km) to the southwest of the site (Figure 12-5). The alluvium is underlain by the Tertiary Wasatch Formation. The weathered upper few feet of the underlying Wasatch Formation also contain unconfined groundwater. Semiconfined and confined groundwater occurs in interlayered sandstone, siltstone, and claystone beds deeper in the Wasatch Formation. The hydraulic gradient in the deeper Wasatch Formation is upward (DOE 1999 [154687], Section 5.2.3). The major ion composition of waters in the unconfined aquifer is quite variable, largely because of seepage of contaminants from site operations. The downgradient groundwaters in the alluvial aquifer are primarily sodium-calcium sulfate waters. Upgradient (background) groundwaters tend to be of the sodium-calcium bicarbonate-sulfate-chloride type, similar to river waters and of much lower ionic strength than downgradient groundwaters (DOE 1999 [154687], Section 5.3.3).

Processing operations at various locations on the site have resulted in the seepage of contaminants into the alluvial aquifer and the upper Wasatch Formation. The major sources of contaminated seepage were the mill and other processing buildings and vats, vanadium and gypsum ponds, evaporation ponds, and the tailings pile (Figure 12-6). The degree to which contaminants have migrated from various source areas on the site has been investigated with an extensive monitoring program that has been in place since 1985. Monitoring wells have been used to obtain water levels and water samples from the alluvial aquifer and from the Wasatch Formation. Monitoring wells that intersect the Wasatch Formation are located within ~0.25 mi of the operations area. The proximity of the uranium source term to the underlying bedrock aquifer

with the upward hydraulic gradient and the disturbed nature of the UMTRA sites are two conditions that would not be analogous to transport at Yucca Mountain.

The locations of the monitoring wells are shown in Figure 12-7. The site-related inorganic constituents most prevalent in the alluvial aquifer include ammonia, calcium, nitrate, molybdenum, selenium, sulfate, and uranium. Of these constituents, the transport behavior of uranium and selenium are of interest to the Yucca Mountain Project. Nitrate and sulfate are potentially of interest as conservative constituents, to trace the maximum extent of movement of contaminants from the site. However, the existence of reducing conditions in various wells downgradient from the site calls into question the use of nitrate as a conservative constituent. Organic constituents such as kerosene were also released to the alluvial aquifer, particularly in and around the processing buildings and vats.

An estimate of the average extent of movement of contaminants from the site, without accounting for dispersion, can be obtained by calculating the distance groundwater could have traveled from the site since operations were initiated in 1958. The estimate is obtained using the following equation for the average linear groundwater velocity, V_x (Fetter 2001 [156668], p. 125):

$$V_x = - K/n_e(dh/dl), \qquad \text{(Eq. 12-1)}$$

where K is the hydraulic conductivity, n_e is the effective porosity, and *dh/dl* is the head gradient.

The average hydraulic conductivity for the New Rifle site is reported as 114 ft/day (0.040 cm/s) (DOE 1999 [154687], Section 5.2.2) was derived for the alluvial aquifer based on pump tests. The effective porosity was specified as 0.27. Based on water-level measurements taken in 1998, the average gradient was found to be 0.0030. Substituting these values into the equation yields the following linear groundwater velocity:

$$V_x = (-114 \text{ ft/day})/0.27(0.0030) = 1.27 \text{ ft/day}$$

A linear groundwater velocity of 1.27 ft/day (0.4 m/day) over a period of 40 years (1958–1998) leads to an estimated travel distance of 18,506 ft (5.64 km).

Because the site operations covered most of the alluvial terrace in a north-south direction and because most of the contamination is in the alluvial aquifer, significant lateral dispersion of contaminated groundwater is precluded by the decreasing width of the alluvial deposits in the downgradient direction. However, the magnitude of the source term for different contaminants may have varied over the site. For example, uranium processing facilities were located in the northern portion of the site. Therefore, uranium concentrations might be expected to be highest in groundwater beneath this portion of the site. In fact, well 655, located near the northern end of the site fence shown in Figure 12-7, has the highest uranium concentrations in any of the wells sampled in the 1998 and 1999 sampling rounds (DOE 1999 [154687], p. 5-56). The absence of similarly high concentrations in downgradient wells suggests the operation of some dispersive process. In addition to lateral dispersion, vertical advective dispersion of contaminants in the alluvial aquifer may also occur. However, the saturated thickness of the alluvial deposits is only 10–20 ft (3–6 m) (DOE 1999 [154687], p. 5-19). Furthermore, the hydraulic gradient in the underlying Wasatch Formation is upward. These observations suggest that vertical advective

dispersion of contaminants in the alluvial aquifer would be limited, but dilution may be an active process.

The use of sulfuric acid in processing ores at the site [inferred to be common practice (Merritt 1971 [156670], p. 29)] would have resulted in seepage to the vadose zone with high concentrations of sulfate. The highest measured concentrations were observed in samples taken in the first two years of the monitoring program. The available data suggest that sulfate concentrations in groundwater beneath and downgradient of the site have generally been decreasing since approximately 1986, consistent with the fact that processing operations at the site ended in 1984. Analyses of groundwater samples from (background) wells in the Wasatch Formation located across the Colorado River and upgradient from the site indicate that these waters have lower sulfate concentrations than waters from the alluvial aquifer but substantially higher chloride concentrations. This suggests the SO_4^{2-}/Cl^- ratio may be useful in identifying groundwaters contaminated by site operations. Groundwaters from wells at background locations (DOE 1999 [154687], Appendix C) show that SO_4^{2-}/Cl^- ratios in the Wasatch Formation are less than 2.0, with most less than 0.5. Water samples from the Colorado River have SO_4^{2-}/Cl^- ratios in the range of 0.75 to 0.85. As shown in Figure 12-8, most water samples from wells located on the site have SO_4^{2-}/Cl^- ratios in the range of 10 to 20. This ratio decreases with distance downgradient. The SO_4^{2-}/Cl^- ratio returns to near-background values at wells 220 and 172, the wells farthest downgradient. Thus, the maximum distance contaminants appear to have traveled from the site, based on the SO_4^{2-}/Cl^- ratio of alluvial groundwater samples, is approximately 19,000 ft (5.8 km). This is similar to the maximum travel distance of 18,506 feet (5.64 km) calculated for groundwater based on hydraulic parameters.

The observed decreases in the SO_4^{2-}/Cl^- ratios (Figure 12-8) and SO_4^{2-} concentrations (6,000 to 2,000 mg/L) in alluvial groundwater with increasing distance downgradient suggests that these waters are progressively diluted with waters that have low SO_4^{2-}/Cl^- ratios and low SO_4^{2-} concentrations. Because there is an upward hydraulic gradient in the Wasatch Formation (DOE 1999 [154687], p. 5-27) and because Wasatch Formation groundwaters from upgradient wells have low SO_4^{2-}/Cl^- ratios (< 0.5) and low sulfate concentrations (< 500 mg/L), the diluting waters most likely come from the Wasatch Formation.

Measured uranium concentrations show a pattern similar to that observed in the SO_4^{2-}/Cl^- ratio data. Upgradient alluvial wells located on the eastern portion of the site have uranium concentrations between zero and 0.05 mg/L (Figure 12-9). Wells located near the former uranium processing buildings on site have the highest uranium concentrations of all water samples (0.4–0.5 mg/L). Note that waters with these uranium concentrations are undersaturated with respect to solid uranyl phases, as calculated by Jove Colon et al. (2001 [157472], p. 13, 14), for groundwater compositions typical of the New Rifle site. Uranium concentrations in alluvial groundwaters decrease downgradient and reach the 0.05 mg/L (background) level between 10,000 and 15,000 ft (3–4.6 km) downgradient (Figure 12-9). Thus, it appears uranium has not traveled downgradient as far as sulfate, although the exact travel distance is difficult to quantify because background values show such a large range (0–0.05 mg/L). The uranium "plume length" based on the 1998 sampling data (3–4.6 km) is considerably greater than the 1 km length proposed by Jove Colon et al. (2001 [157472], p. 24) as the "steady-state" length for uranium plumes in groundwater systems (i.e., the length at which uranium concentration in monitoring wells remains fairly constant). In fact, there is no evidence in the New Rifle data that the

uranium migration rate has decreased significantly with time, contrary to the conclusions reached by Jove Colon et al. (2001 [157472], p. 24).

Taking the maximum distance traveled by uranium as 13,000 ft (Figure 12-9) and the maximum distance traveled by sulfate as 18,000 ft (Figure 12-8), an estimated retardation factor (R_t) for uranium of 1.38 (i.e., 18,000/13,000) is obtained. Using the retardation equation (Freeze and Cherry 1979 [101173], Equation 9.14)

$$R_t = (1 + \frac{\rho_b K_d}{\phi}), \qquad \text{(Eq. 12-2)}$$

where ρ_b is the dry bulk density in g/cm^3 and ϕ is the porosity, we can solve for the sorption coefficient (K_d),

$$K_d = \frac{(R_t - 1)\phi}{\rho_b}. \qquad \text{(Eq. 12-3)}$$

Using values for the dry bulk density (ρ_b) and porosity given for the alluvial aquifer in DOE (1999 [154687]), we obtain the following result for the uranium sorption coefficient (K_d):

$$K_d = (1.38 - 1)0.25/1.52 = 0.06 \text{ mL/g}.$$

Batch-sorption coefficient measurements for uranium using alluvial materials from the New Rifle site and a synthetic groundwater show a range of coefficients from -0.3–1.4 mL/g, with an average value of 1.0 mL/g (DOE 1999 [154687], Table 4-6). The K_d calculated here falls within that range, but is lower than the mean average value. This difference may be partly accounted for by the fact that the calculated R_t is based on what may be closer to the maximum, rather than the average, distance traveled by uranium; therefore, the calculation yields a lower K_d.

It is possible also that some uranium could have been transported downgradient as part of a colloidal phase (including microbes). Such colloidal transport could carry the uranium at essentially the velocity of groundwater. As part of the Nye County Early Warning Drilling Program, several monitoring wells have been installed down gradient of the potential repository at Yucca Mountain. Colloid transport is being studied through analyses of groundwater samples collected from these wells (Kung et al. 2001 [157604]).

Selenium has been detected only in groundwaters from wells located within the boundaries of the original New Rifle site. There is no evidence of significant downgradient transport. This is probably a result of the combined effects of a smaller source term and higher sorption coefficients measured for selenium in contact with sediments from the alluvial aquifer (DOE 1999 [154687], pp. 5-41, 5-42).

In summary, the data available on uranium transport at the New Rifle UMTRA site suggest that dilution in the alluvial aquifer is a significant process downgradient from the site and that the sorption of uranium on alluvial sediments also occurs.

12.3.3.3 Summary and Conclusions of UMTRA Study

An evaluation of data available for 24 UMTRA sites determined that only a few of these sites are potentially useful in the evaluation of transport of radionuclides in the alluvial portion of the Yucca Mountain flow system. Most of the sites are of limited use either because they are situated in a hydrogeologic setting different from Yucca Mountain or because there is insufficient information available to perform an adequate evaluation of transport behavior. There are enough data available for the Gunnison and New Rifle sites to perform a useful analysis. The conclusions derived from an analysis of the Gunnison site are (1) that a fraction of the uranium originating at the site is transported in the alluvial aquifer at a rate similar to the rate at which a conservative constituent is transported, and (2) there is little evidence for dispersion of contaminants in the downgradient direction. For the New Rifle site, the main conclusions are (1) that dilution is a significant process in the downgradient direction and (2) that uranium is transported at a slower rate then conservative constituents, although a fraction of the uranium traveled almost as far. The conclusions regarding uranium transport distances relative to conservative constituents must be tempered somewhat by uncertainties regarding the potential presence of unidentified complexing agents, such as organic materials, that could form colloids and enhance uranium transport. An additional note of caution attaches to the use of laboratory batch-derived K_d values for the prediction of large-scale field transport, because the two parameters are conceptually and numerically different.

12.4 OTHER SATURATED ZONE ANALOGUES

12.4.1 Uranium Retardation under Oxidizing Conditions

Studies of the weathered zone overlying the Coles Hill, Virginia, uranium deposit indicate that the natural attenuation of uranium in oxidizing environments may occur in groundwaters with low dissolved carbonate/phosphate ratios (Jerden and Sinha 2001 [157474]). At the Coles Hill site, uranium concentrations are buffered to values <20 ppb due to the precipitation of low-solubility U(VI) phases. The attenuation mechanism involves the transformation of U(IV) coffinite, the primary ore, to U(VI) phosphate minerals. Above the water table in the soil zone, where phosphate minerals are rare, uranium is primarily associated with an aluminum phosphate of the crandallite mineral group and with phosphorous sorbed to ferric hydroxide mineral coatings. Experiments demonstrated that the transformation of U(IV) to U(VI) assemblages could occur in less than two months, given high enough phosphate levels. Model predictions agreed with the field observations: for oxidizing systems with relatively low dissolved carbonate/phosphate ratios, uranium may be immobilized by secondary uranium phosphate precipitation and sorption processes. It is unlikely that low dissolved carbonate/phosphate ratios would occur in bedrock aquifers at Yucca Mountain, but if use of phosphate-containing fertilizer contaminates the alluvial aquifer in Amargosa Valley, the carbonate/phosphate ratio could be lowered, making this a more analogous situation for Yucca Mountain.

12.4.2 Matrix Diffusion

12.4.2.1 El Berrocal

El Berrocal is an area approximately 100 km southwest of Madrid, Spain. The El Berrocal granite forms a large hill and contains a number of small, vein-hosted uranium ore bodies, one of which was the focus of analogue investigations (Figure 12-10). The El Berrocal granite has a uranium content that averages 16 mg/kg, with primary uranium occurring as accessory uraninite dispersed in the granite matrix (De la Cruz et al. 1997 [157473], pp. 82–83). Post-emplacement hydrothermal alteration mobilized some of the uranium, thorium, and rare-earth elements from the granite and redeposited them in a 2-m-wide, steeply dipping quartz vein more than 1 Ma (Rivas et al. 1998 [126287], pp. 15–16). Erosion and weathering exposed the vein-hosted mineralization, causing further elemental mobilization and transport. The groundwaters contain moderate to low concentrations of uranium (4×10^{-9} to 8×10^{-6} M) (De la Cruz et al. 1997 [157473], p. 81; this converts to 9.52×10^{-4} to 1.9 mg/L). Carbonate complexes are the dominant species in oxidized zones and U(IV) hydroxides in reduced zones. The general behavior of uranium can be accounted for by the kinetic control of the dissolution of the source term and solubility controlled by coprecipitation processes.

The multinational El Berrocal project had the objective of investigating these present-day, low-temperature processes, as well as the processes responsible for elemental retardation in the granite. In particular, the study investigated uranium mineral stability, degradation, and dissolution; uranium solubility and speciation; matrix diffusion in the rock adjacent to fractures, and colloidal transport of radionuclides. Study activities included blind predictive testing of geochemical codes and databases. The results of the project indicated that mobilized uranium and thorium tended to be associated by sorption and coprecipitation with certain fracture-coating minerals, notably iron oxyhydroxides and calcite. Enrichment of uranium by a factor of up to 6 was observed, and up to 3 for thorium, relative to the unaltered granite (Miller et al. 2000 [156684], p. 201). Considerable effort was made to understand these coprecipitation processes in order to improve thermodynamic models and databases for performance assessment (Section 15).

12.4.2.2 Matrix Diffusion Comparison Studies

The Palmottu, Finland, site in saturated, fractured gneisses and migmatites was the location of a matrix diffusion study. Radionuclide concentration profiles from a fracture in the rock matrix were examined in several different drillcores (Blomqvuist et al. 1995 [124640]). Alpha-autoradiography showed the distribution of radionuclides decreasing from the fracture surface into the rock matrix. Based on the findings of three drillcore samples, the profile of decreasing radioactive content could be traced >100 mm into the rock (Blomqvist et al. 1995 [124640], pp. 64–65). The radionucides were associated with clay particles and iron oxyhydroxides that had formed from alteration of feldspar and biotite grains. Selective leaching experiments showed that most of the radionuclides that had diffused into the rock matrix were only loosely bound to the iron-rich phases. In some samples, activity correlated to microfractures indicated that fluid flow was channelled even at the microscopic level, whereas in another sample diffusion was predominantly along grain boundaries. This supports the hypothesis that physical disruption around a fracture may enhance transport into the rock matrix (Blomqvist et al. 1995 [124640], pp. 27, 60, 63, 64).

A comprehensive investigation of matrix diffusion processes compared granite samples from a number of locations: the El Berrocal natural analogue site, Spain; the Stripa test mine, Sweden; the Whiteshell Underground Research Laboratory (URL), Canada; and the Grimsel Test Site, Switzerland (Heath 1995 [157478]). Each sample was taken from close to a hydraulically active fracture, cut to provide a series of slices parallel to the fracture, and characterized in detail. For all samples, the region of enhanced uranium mobility correlated with the zone of microstructural alteration in the rock adjacent to the fractures. The actual depth of enhanced uranium mobility varied from site to site; for instance, enhanced uranium mobility extended 35 mm in the shallow El Berrocal granite, but 50 mm in both the altered and unaltered URL granite.

Interpretation of the El Berrocal core sample data indicated the following: not only was matrix diffusion limited to the first few tens of millimeters of rock adjacent to the fracture surface, but also within the rock matrix the mobilized uranium was associated with secondary phases and located in microfissures along grain boundaries (Heath 1995 [157478], p. 51). There was a very good correlation between the distribution of the mobilized uranium, the redox conditions, and the isotopic disequilibrium. Heath (1995 [157478], p. 51) concluded from a combination of all of the data that a complex combination of matrix diffusion and chemical interaction had occurred between the rock and the mobile phases, rather than matrix diffusion alone. From this conclusion, Heath suggested the possibility that retardation processes that rely on matrix diffusion mechanisms may make little overall contribution to performance in a crystalline rock mass. However, the data from El Berrocal provide good evidence that, once radionouclides migrate into the rock matrix from the flowing fracture, they are effectively immobilized irrespective of the process involved.

12.4.3 Colloidal Transport in the SZ

Colloids are ubiquitous in all groundwaters (McCarthy 1996 [157479], p. 197). However, in deep crystalline rocks with a stable geochemical system, the colloid populations are low, ~25 µg/L. In contrast, shallow aquifer systems generally appear to have the largest colloid populations, even in the absence of geochemical stability. Enhanced colloidal populations occur in all rock types where there is some hydrogeochemical perturbation to the system. For example, in fractured granitic systems, colloid populations are 20 to 1,000 times higher in groundwaters affected by inputs of surface water or in hydrothermal zones with large temperature and pressure gradients, compared to stable hydrogeochemical systems (Degueldre 1994 [101128]).

The uptake and transport of radionuclides by colloids has been investigated in several analogue studies of natural systems with enhanced radionuclide content: Cigar Lake, Canada (Vilks et al. 1993 [108261]); Alligator Rivers, Australia (Seo et al. 1994 [157480], p. 75); El Berrocal, Spain (Rivas et al. 1998 [126287]); and Poços de Caldas, Brazil (Miekeley et al. 1992 [106762]). In most of these studies, it was found that some proportion of the total uranium, thorium, and rare-earth elements in the groundwater was associated with the colloids. This proportion was higher for thorium than for uranium because of thorium's lower solubility in most groundwaters. The rare earths generally show an affinity for colloids intermediate between uranium and thorium (Miekeley et al. 1992 [106762], pp. 429, 434).

Unambiguous evidence from natural systems indicating colloidal transport over long distances is rare. The only known example suggesting transport on the kilometer scale is at Menzenschwand,

Germany, where the Ti:Mg ratio and rare-earth-element composition of the natural colloids differed from that of the host granite but were similar to that of a neighboring gneiss several kilometers away and upgradient (Hofmann 1989 [125081], pp. 925–926). However, the flow system at Menzenschwand is not representative of a natural system, because it is perturbed by the presence of a uranium mine with associated fast flow.

Many analogue studies suggest that colloid transport in natural systems is significantly restricted. For instance, at Cigar Lake, the uranium and radium contents of colloids in the ore and the surrounding clay zones are significantly higher than in colloids from the sandstone host rock, indicating that the clay is an effective barrier to colloid migration (Vilks et al. 1993 [108261]). Similar results at Alligator Rivers and Morro de Ferro also suggest that colloids have a limited capacity for migration, because the concentrations of colloid-bound radionuclides outside the orebodies are relatively low (Miekeley et al. 1992 [106762], pp. 420, 432–433).

Colloid concentrations of 0.8–6.9 mg/L for particles greater than 30 nm were observed in two wells on Pahute Mesa at the Nevada Test Site (NTS) (Buddemeier and Hunt 1988 [100712], p. 537). One well was inside the Cheshire experimental site, and the second, a water well, was 300 m away. Tritium, krypton, strontium, cesium, antimony, cobalt, cerium, and europium were detected in pumped water from the water well. All of the cobalt, cesium, and europium were associated with colloids in samples from both locations. Buddemeier and Hunt (1988 [100712], p. 537) maintained that the presence of colloidal radionuclides outside the cavity indicates radionuclide transport as colloids.

In another study at the NTS (Kersting et al. 1999 [103282], p. 56), isotopic ratios of plutonium were used to fingerprint the source of plutonium detected in monitoring wells with a specific underground nuclear test, suggesting that the plutonium migrated a distance of 1.3 km. Plutonium has a tendency to strongly sorb to tuff minerals, which would retard its transport. Thus the observed presence of colloids in waters at the NTS and the observed association of plutonium with colloids were interpreted to indicate that radionuclide transport was expedited by colloids.

A similar conclusion was reported by Triay et al. (1997 [100422], p. 172) to explain the transport of plutonium and americium away from a low-level waste site in alluvial sediments at Mortandad Canyon at Los Alamos, New Mexico. These radionuclides were detected at depths of 30 m in monitoring wells in unsaturated tuff up to 3.4 km downgradient from the waste disposal site (Buddemeier and Hunt 1988 [100712], p. 536). The migration reportedly took place over a period of 30 years (Buddemeier and Hunt 1988 [100712], p. 536). Because sorption studies involving the alluvial sediments suggested that plutonium and americium should be relatively immobile, the observed movement of radionuclides was reported by Triay et al. (1997 [100422], p. 172) to suggest that the transport of plutonium and americium through alluvium resulted from association with highly mobile colloids.

These observations lend support to the concept that radionuclide transport in the far field can be facilitated by colloids, but so far no natural analogue studies have been able to quantify the importance of this process.

12.5 CONCLUSIONS

UMTRA Study: Only a few of the UMTRA sites are potentially useful in the evaluation of radionuclide transport in the alluvial portion of the Yucca Mountain flow system. Most of the sites are of limited use either because they are situated in a hydrogeologic setting different from Yucca Mountain or because there is insufficient information available to perform an adequate evaluation of transport behavior. Enough data were available for the Gunnison and New Rifle sites to perform a useful analysis. The conclusions derived from an analysis of the Gunnison site are: (1) a fraction of the uranium originating at the site is transported in the alluvial aquifer at a rate similar to the rate at which a conservative constituent is transported, and (2) there is little evidence for lateral dispersion of contaminants in the downgradient direction. For the New Rifle site, the main conclusions are: (1) dilution is a significant process in the downgradient direction, and (2) uranium is transported more slowly than conservative constituents. The conclusions regarding uranium transport rates relative to conservative constituents must be tempered by uncertainties regarding the potential presence of unidentified complexing agents.

Diffusion: Matrix diffusion in crystalline rock is generally limited to only a small volume of rock close to fractures, but even a small volume can make a significant difference in radionuclide retardation.

Sorption onto fractures: Comparison of the results from a number of analogue study sites shows that similar sorption behavior is seen at many locations in crystalline rocks. For example, uranium and rare earth elements are frequently associated with calcite and iron oxyhydroxides. However, because it is often impossible to define in detail the paleohydrological history of a site, it is difficult to identify the unique effects of recent low-temperature retardation events. This is possibly the reason for the anomalous observations at El Berrocal related to limited observed uranium sorption on iron oxyhydroxides.

Although several natural analogue studies have demonstrated the effect of sorption and precipitation processes on fracture surfaces, none has been able to distinguish clearly between these processes or to provide quantitative data on retardation with respect to transport of trace elements in natural waters. However, these studies do highlight which phases are most active, and they provide useful information on the effect of interaction between solutes and the rock surface.

Colloid transport: In most studies of natural systems, it was found that some portion of the total uranium, thorium, and rare-earth elements in the groundwater was associated with colloids. Unambiguous evidence from natural systems indicating colloidal transport over kilometer-scale distances is limited to a few reports. Observations from such places as Los Alamos and the NTS lend support to the concept that radionuclide transport in the SZ can be facilitated by colloids, but so far no natural analogue studies have been able to quantify the importance of this process.

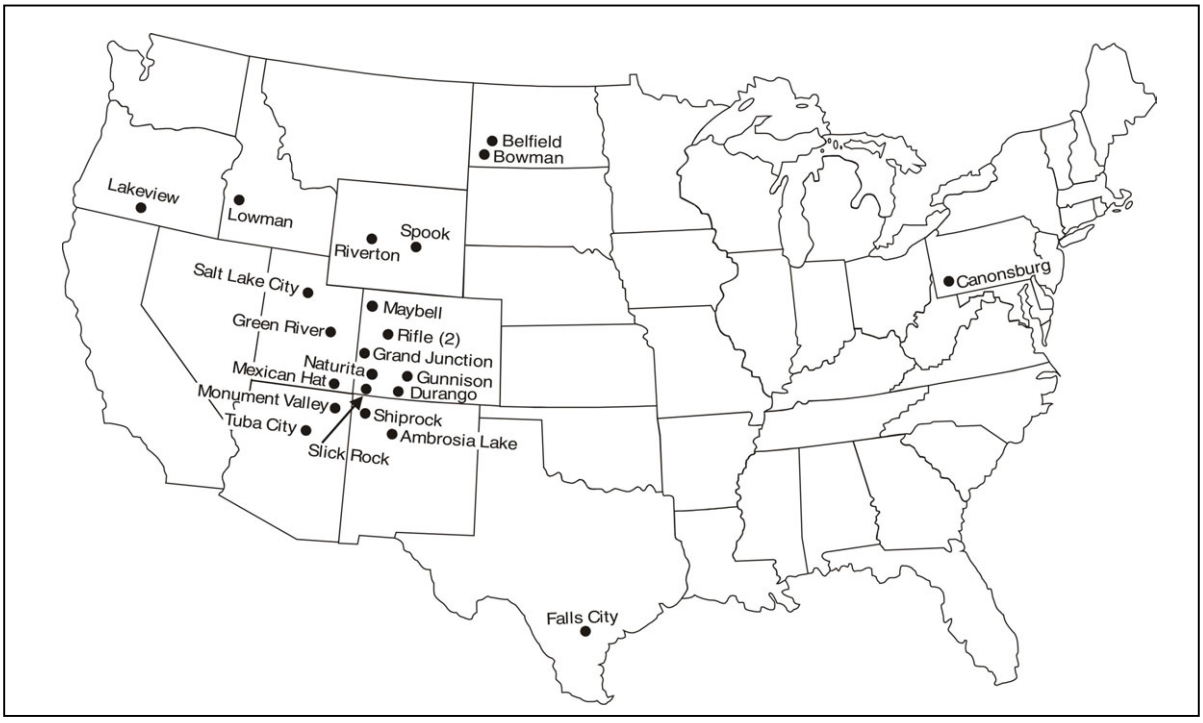

Source: Modified from DOE 2000 [157603].

Figure 12-1. Locations of UMTRA Ground Water Project Sites

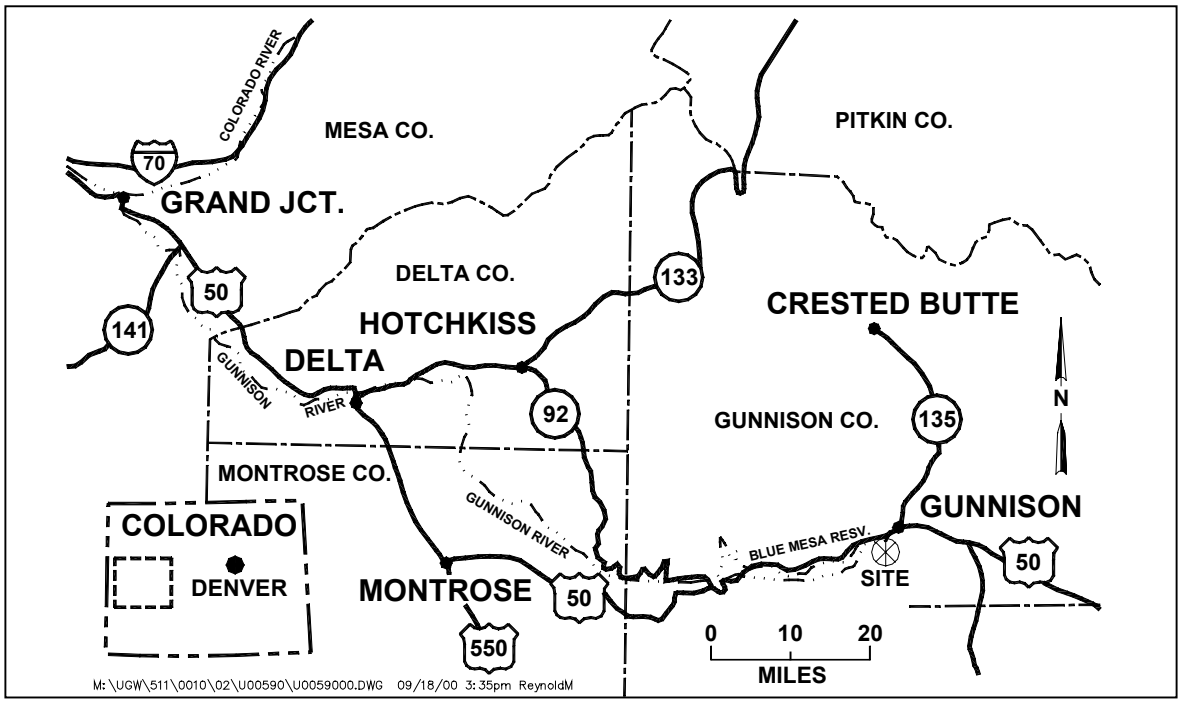

Source: DOE 2001 [156666], Figure 1-1.

Figure 12-2. Location Map for Gunnison UMTRA Site

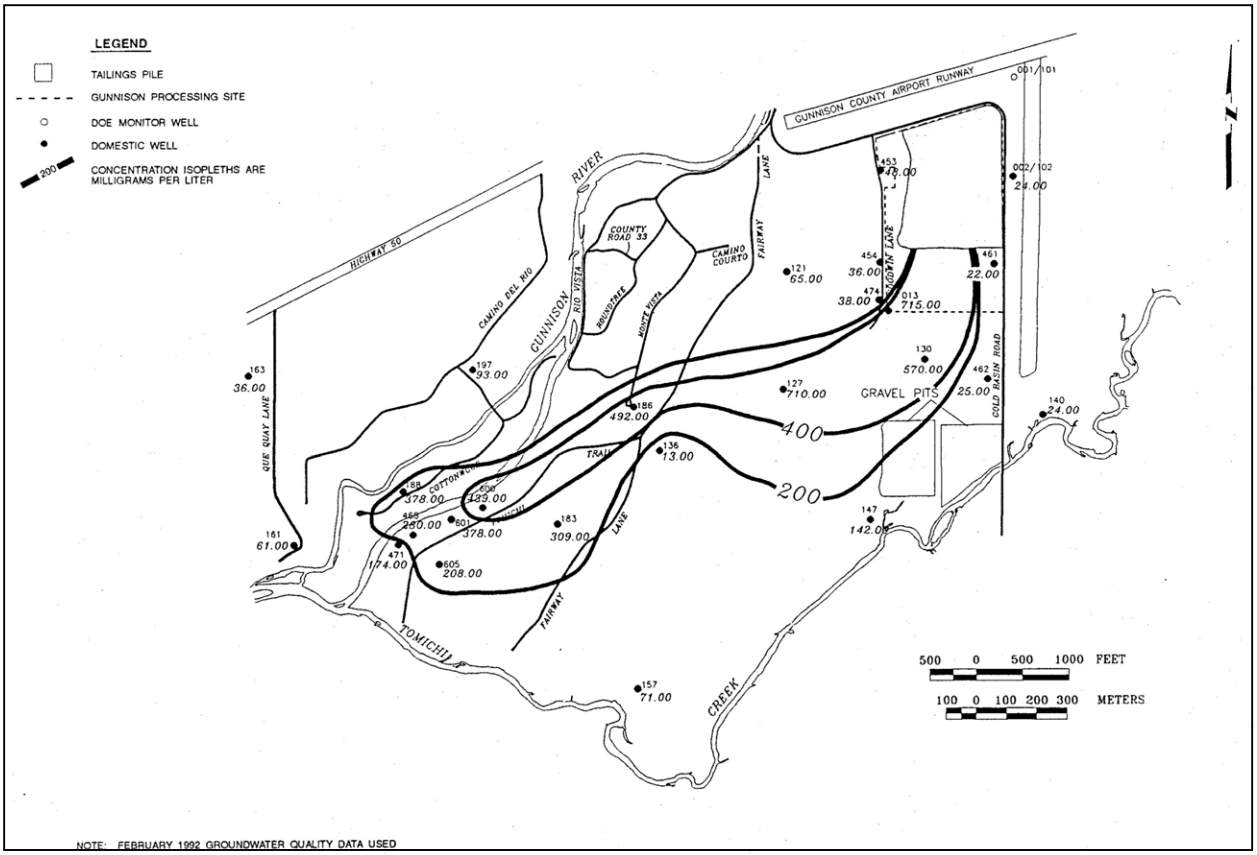

Source: DOE 1992 [154692], Figure 3.10.

Figure 12-3. Plume Map of Sulfate Concentrations (mg/L) in Alluvial Groundwater at Gunnison UMTRA Site

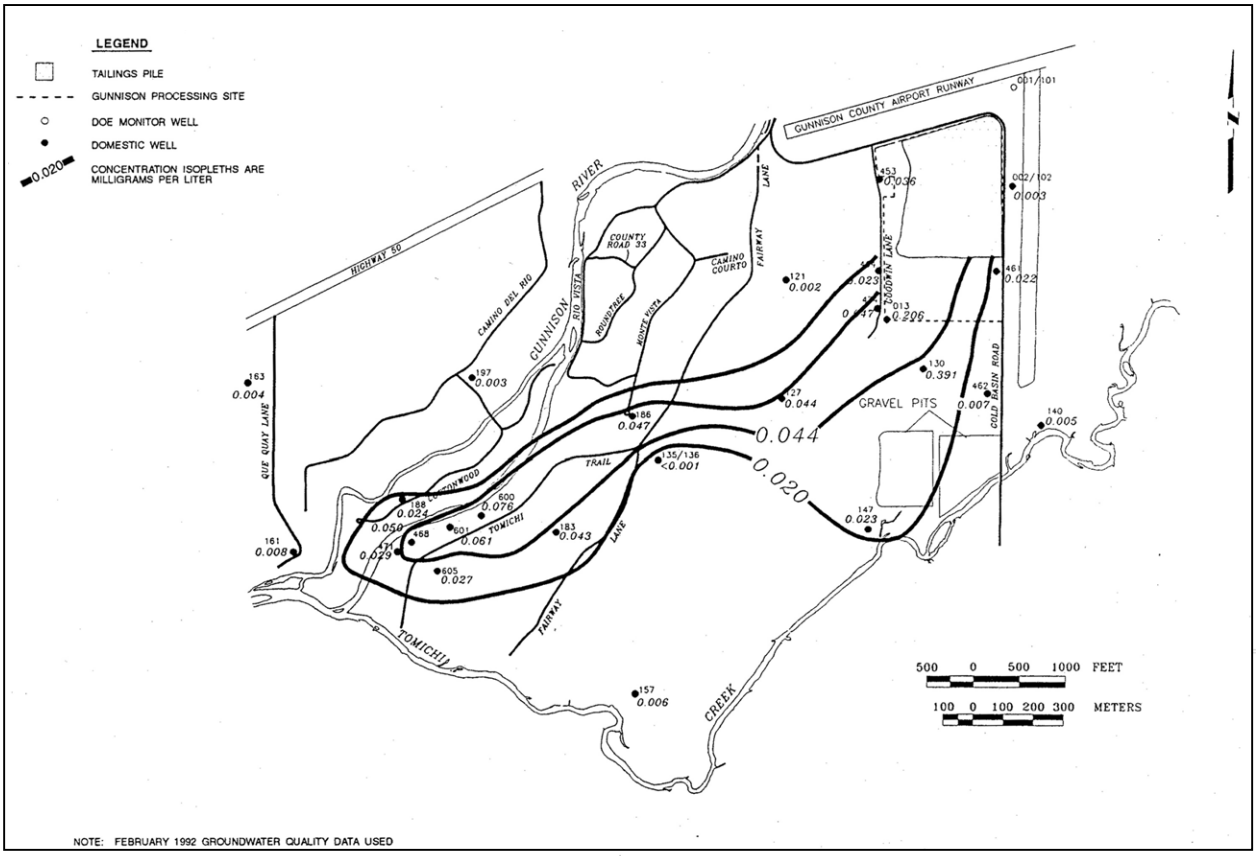

Source: DOE 1992 [154692], Figure 3.12.

Figure 12-4. Plume Map of Uranium Concentrations (mg/L) in Alluvial Groundwater at Gunnison UMTRA Site

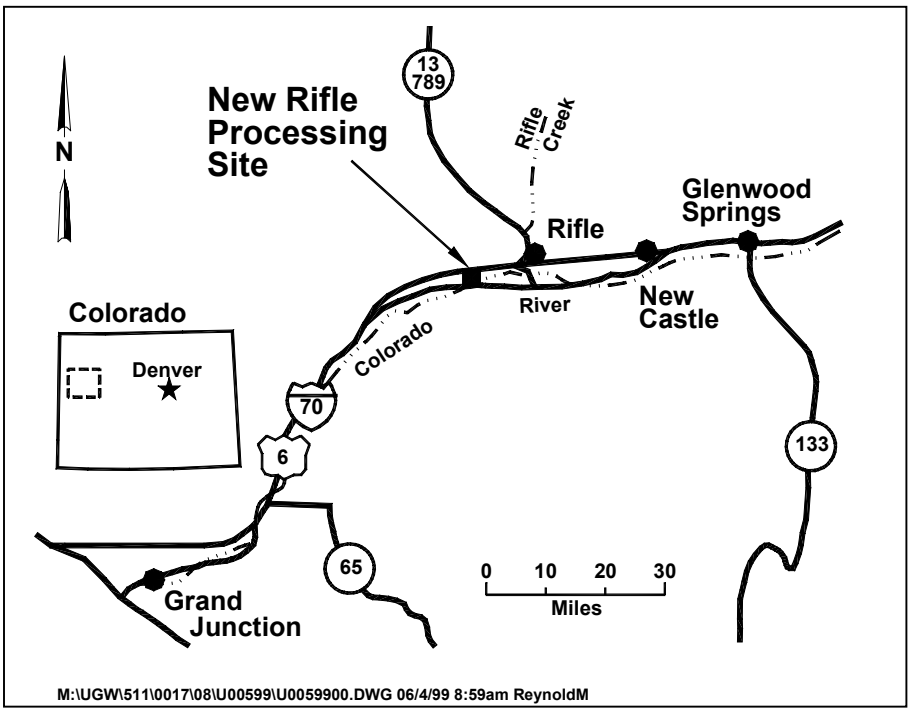

Source: DOE 1999 [154687], Figure 1-1.

Figure 12-5. Location Map for New Rifle UMTRA Site

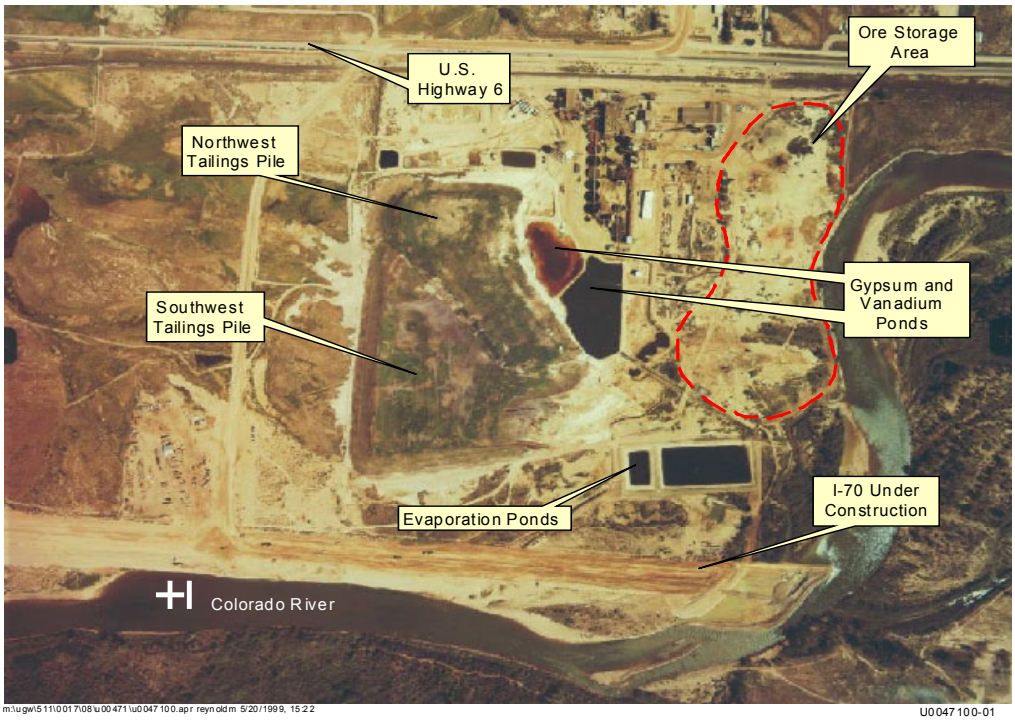

Source: DOE 1999 [154687], Figure 3-1.

Figure 12-6. Aerial Photo of New Rifle UMTRA Site, Showing Location of Tailings Piles (August 1974)

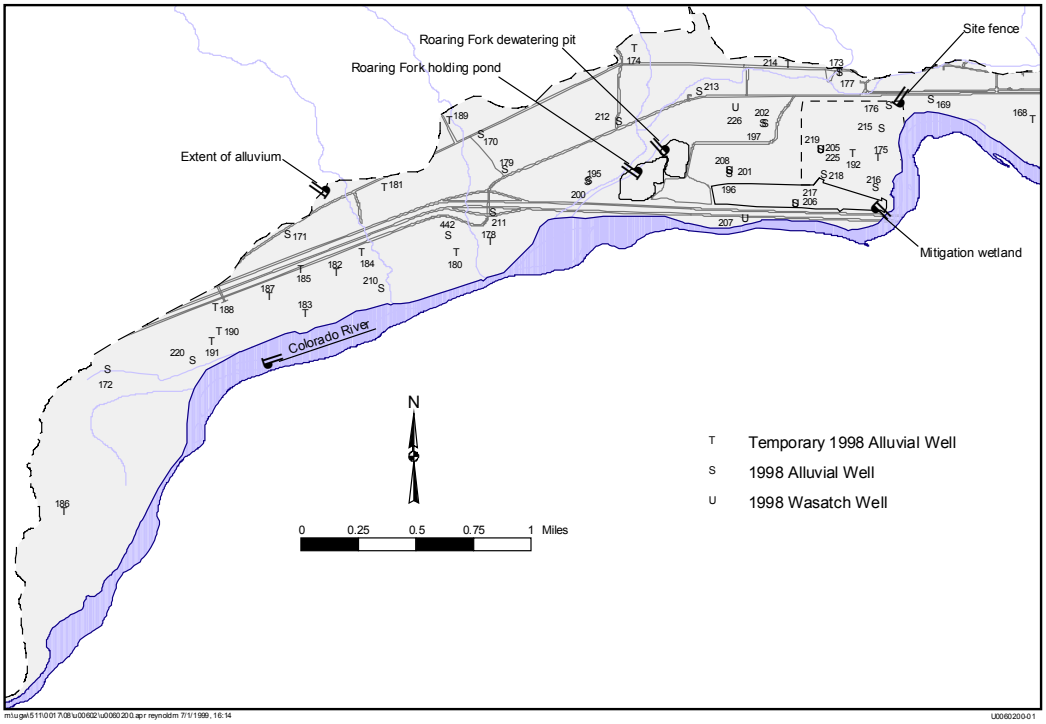

Source: DOE 1999 [154687], Figure 4-1.

Figure 12-7. Map Showing Locations of Wells Screened in Alluvial Aquifer at the New Rifle UMTRA Site

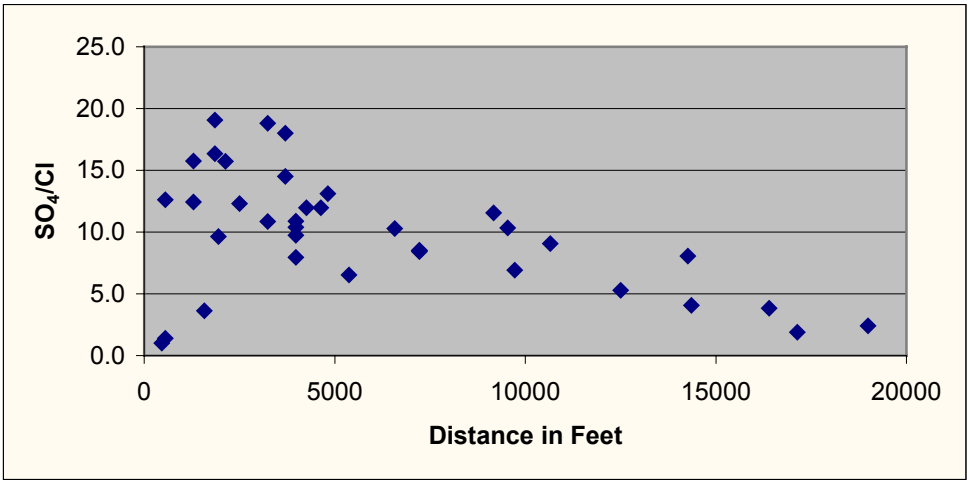

Source: DOE 1999 [154687], Appendix C.

Figure 12-8. Sulfate/Chloride Ratios in Downgradient Alluvial Groundwater versus Distance in Feet from Colorado River Bank on Eastern Edge of New Rifle UMTRA Site

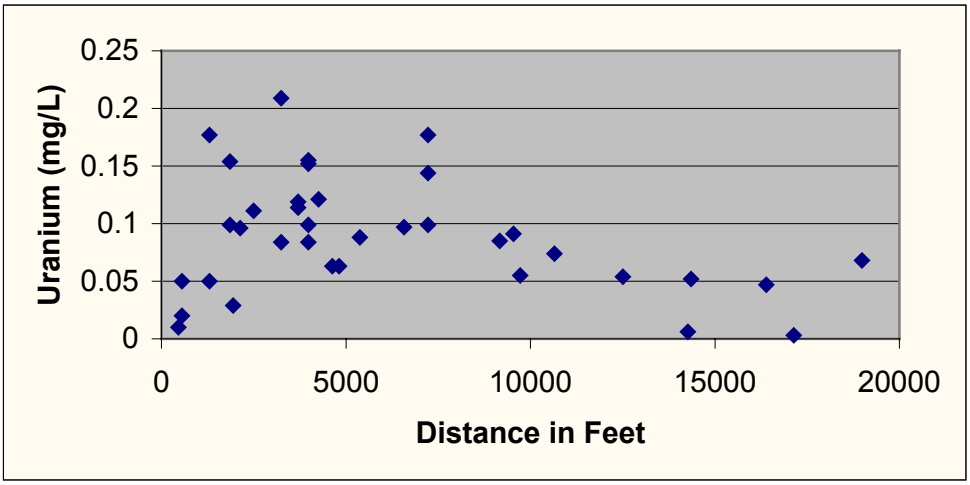

Source: DOE 1999 [154687], Appendix C.

Figure 12-9. Uranium Concentration in Downgradient Alluvial Groundwater versus Distance in Feet from Colorado River Bank on Eastern Edge of New Rifle UMTRA Site

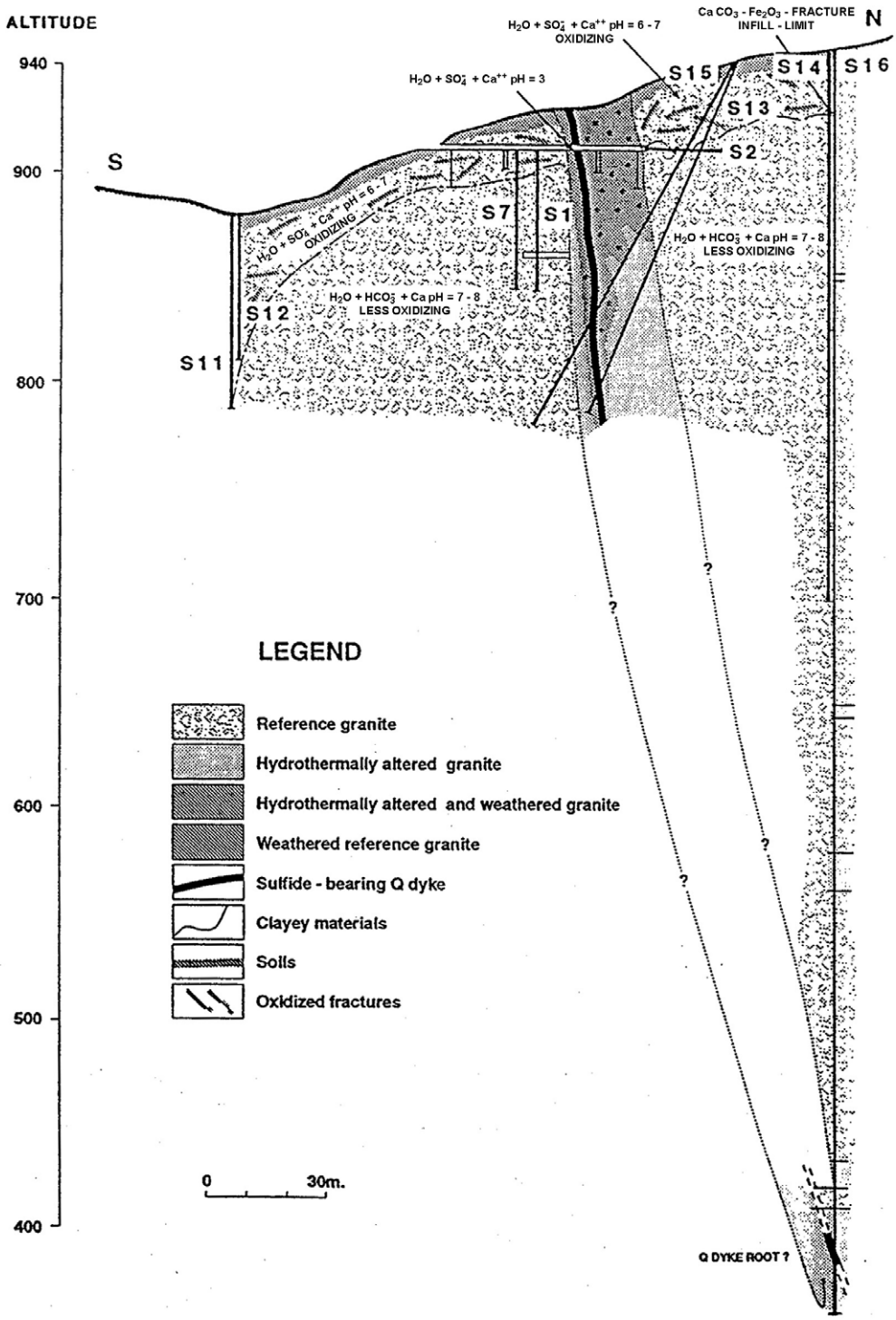

Source: Rivas et al. 1998 [126287], Figure 2-1.

Figure 12-10. N-S Cross Section of the El Berrocal Granite-Uranium-Quartz-Vein System and Location of Selected Boreholes

13. ANALOGUE INFORMATION FOR BIOSPHERE PROCESS MODELS

13.1 INTRODUCTION

Section 13 presents information from the Chernobyl Nuclear Power Plant (ChNPP) accident in Ukraine that relates to parameters of interest in the Yucca Mountain Biosphere Process Model. Unlike the analogues presented in previous sections that dealt primarily with demonstrating confidence in processes and conceptual models, analogues relevant to biosphere models tend to focus on parameter input values. In Section 13.2, the Biosphere Process Model is briefly described to provide background against which to assess its information needs. Section 13.3 focuses on studies of the Chernobyl nuclear accident and its consequences to the biosphere, and their pertinence to the Yucca Mountain Biosphere Process Model.

Although there are many contaminated sites that might have been suitable candidates for providing analogue information for the Biosphere Process Model, Chernobyl was selected for an in-depth survey. Chernobyl provides several advantages over other contaminated sites. First, the Chernobyl site was studied extensively after the 1986 accident, and a wealth of data has been published. Second, because the Chernobyl accident involved an explosion, data regarding the settling of contaminants following atmospheric transport resulting from the explosion provide a rather unique opportunity for use in adding confidence to the disruptive-event-pathway component of the Yucca Mountain Biosphere Process Model.

13.2 BACKGROUND

13.2.1 Reference Environmental Conditions for the Yucca Mountain Biosphere Process Model

The Yucca Mountain reference biosphere conceptual model is based on the biosphere environmental setting, including geography, climate, hydrogeology, geology, and soil conditions, as well as ecosystems (including human communities) (CRWMS M&O 2000 [151615], Section 3.1.1). Yucca Mountain is located in a sparsely populated, semi-arid region in the transition zone between the Great Basin and the Mojave deserts. Yucca Mountain and surrounding areas are in the southern part of the Great Basin, the northern-most subprovince of the Basin and Range Physiographic Province. The topography, which is typical for the Great Basin, is characterized by relatively regularly spaced mountain ranges and intervening alluvial basins, trending from the north to the south. The mountain ranges are formed by fault blocks that are tilted eastward, so that the fault-bounded west-facing slopes are generally high, steep, and straight, in contrast to the gentler and deeply dissected east-facing slopes.

Yucca Mountain has low annual precipitation (from 100 to 200 mm) that decreases from the higher to lower elevations. About 50% of the annual precipitation falls from November through April, caused by large frontal storms. Summers are hot and winters are cool. The Sierra Nevada Mountains that lie to the west create a major barrier to moist air masses moving from the Pacific Ocean. Some thunderstorms in summer are able to create localized land surface flooding and runoff. The average maximum daytime temperature varies from 11°C (52°F) in January to 35°C (95°F) in July. Average nighttime temperatures are above freezing in January (2°C

[36°F]), but winter freezing may occur. Average annual atmospheric humidity is less than 20%. Such conditions cause high evapotranspiration. Vegetation covers 20 to 30% of the ground, with shrubs dominating the native vegetation.

The nearest settlement to Yucca Mountain is situated in the direction of groundwater flow in Amargosa Valley (Nye County). Amargosa Valley is an area of approximately 1,300 km^2. The closest inhabitants to Yucca Mountain are approximately 20 km south at the intersection of U.S. 95 and Nevada State Route 373. The Amargosa Valley population is about 1,270, in approximately 450 households. The Amargosa Valley region is primarily rural agrarian in nature, with agriculture mainly directed toward growing livestock feed (e.g., alfalfa), gardening, and animal husbandry. Both the agriculture and the population are concentrated in the Amargosa Farms area, approximately 30 km south of Yucca Mountain. Agricultural crops and gardens depend entirely on irrigation. Because there is no natural discharge of groundwater into the Amargosa Valley, the source of water for household uses, agriculture, horticulture, and animal husbandry is from local wells. Thus, the pathway for introduction into the biosphere is the use of wells for residential and agricultural purposes.

The direction of groundwater flow is from north to south, with a discharge into the Amargosa Valley region located immediately to the south of Yucca Mountain. If radionuclides were to be released into groundwater or air at Yucca Mountain, groundwater flow and wind patterns could spread some contaminants into this region over time.

Sandy-textured soils are found in Amargosa Valley. The active soil depth is 15 cm, in which deposition from the atmosphere, irrigation, and resuspension may occur. The soil bulk densities in farming areas of Amargosa Valley range from 1.35–1.70 g/cm^3, with a mean value of 1.5 g/cm^3 used in the Yucca Mountain Biosphere Process Model (CRWMS M&O 2000 [151615], Section 3.2.4.1.3).

13.2.2 Biosphere Process Model Pathways

The Biosphere Process Model describes exposure pathways in the biosphere by which radionuclides released from a potential Yucca Mountain repository could reach a human receptor (Figure 13.2-1). The Yucca Mountain biosphere conceptual model considers two scenarios of possible radionuclide releases (CRWMS M&O 2000 [151615], Section 3.1.5). The first scenario assumes pumping of contaminated groundwater and use of this water in a hypothetical farming community (a) under undisturbed repository performance and (b) for some disruptive processes and events, such as volcanic activity, or through human activities such as drilling a borehole through a degraded waste container. Under the contaminated-groundwater scenario, infiltration through the unsaturated zone (UZ) or along a borehole would enable radionuclides to reach the saturated zone (SZ), followed by lateral spreading of radionuclides and pumping of contaminated groundwater. In this case, radionuclide-contaminated groundwater is used as the source of drinking water, irrigation, animal watering, and domestic uses (including gardening), thus increasing the likelihood of uptake by humans. The second scenario assumes that the release is caused by a volcanic discharge through the repository, leading to atmospheric dispersal of the contaminants into the accessible environment through ash fall, which accumulates on the land surface. These contaminants may then be absorbed by plants and digested by animals, thus

entering the food chain and being made available for human consumption. Groundwater is assumed to be uncontaminated in the disruptive volcanic-event scenario.

The Yucca Mountain Biosphere Process Model develops biosphere dose conversion factors (BDCFs), which are multipliers used in Total System Performance Assessment (TSPA) to convert the radionuclide concentration at the source of contamination into an annual dose, as defined by the regulator. For the groundwater-contamination scenario, annual doses are estimated by multiplying radionuclide concentrations in groundwater by the corresponding BDCFs. For the disruptive event scenario that results in a surface-contaminated source term, the doses are obtained by multiplying surface-activity concentration of a radionuclide by the corresponding BDCF (CRWMS 2000 [151615], Section 3.1.4).

13.3 USING CHERNOBYL DATA FOR EVALUATING BIOSPHERE PATHWAYS OF RADIONUCLIDES

13.3.1 Relevance of Chernobyl Information

Information about the distribution of radionuclides in the biosphere following the Chernobyl Nuclear Power Plant (ChNPP) reactor explosion in April 1986 is a valuable source of data for testing environmental transport models (Hoffman et al. 1996 [156616]; Konoplev et al. 1999 [156624]). The 1986 Chernobyl accident resulted from an explosion of the Fourth Reactor Unit of the ChNPP. Figure 13.3-1 shows the location of the ChNPP in the territory of Ukraine. The ChNPP accident resulted in contamination by a variety of radionuclides (^{89}Sr, ^{90}Sr, ^{95}Zr, ^{99}Mo, ^{103}Ru, ^{106}Ru, ^{134}Cs, ^{137}Cs, ^{141}Ce, ^{144}Ce, ^{154}Eu, ^{155}Eu, ^{238}Pu, ^{239} Pu, ^{240}Pu, ^{241}Pu, etc.) of large areas of the former USSR and the globe (Bar'yakhtar 1997 [156953], p. 35; Kashparov 2001 [156819], p. 11). Research into many environmental and health effects of the Chernobyl accident has become a major international enterprise aimed at understanding long-term transport processes and effects of exposure to radioactivity. A significant amount of data has been collected for the past 16 years about the distribution and accumulation of radioactive materials in different parts of the biosphere after the Chernobyl accident, including the main exposure pathways and mechanisms of radioactive contamination of the environment and the population. These data represent a valuable source of information to improve confidence in conceptual models of exposure pathways and processes.

13.3.2 Objective and Approach

Because direct observation of the actual outcome of the Biosphere Process Model scenarios will not be possible for many years, if ever (CRWMS M&O 2000 [151615], Section 3.2.3), one of the approaches to building confidence in biosphere models is to use information obtained from natural and anthropogenic analogue sites. As part of the model validation activities to improve biosphere models for both the groundwater-release and the volcanic-release scenarios, the Yucca Mountain Project is interested in measurements at specific locations to aid in selection of input data for models of specific environmental processes.

The objective of Section 13.3 is to review information from the Chernobyl accident regarding the exposure pathways, inputs to risk assessment, and distribution of radioactive contaminants in the biosphere, to determine its potential relevance for the Yucca Mountain Biosphere Process Model.

In particular, information was collected on the specific environmental processes of radionuclide transfer and resuspension, which could be used to improve confidence in the modeling of Yucca Mountain environmental processes. Major monographs and numerous articles were reviewed in English, Russian, and Ukrainian scientific and professional journals, magazines, and proceedings of international conferences and symposia.

Taking into account the difference in climatologic and environmental conditions of Chernobyl and Yucca Mountain, this survey presents a broad picture of the environmental pathways of radionuclides in the biosphere. Radiation doses resulting from Chernobyl are presented as a means of illustrating the types of data available related to stated needs of the Yucca Mountain Biosphere Department, including the following:

- Radionuclide transfer from soil to plants via root uptake, soil to plants via atmospheric resuspension, and animal fodder to animal food products
- Removal of contaminants via erosion and leaching
- Inhalation of resuspended contaminants deposited on the ground
- Radionuclide accumulation in soils and plants under irrigation using contaminated water
- The ecological half-life of radionuclides in soils and plants.

13.3.3 Chernobyl Accident and Main Exposure Pathways

This section provides background for later discussion by describing the Chernobyl location, climate, and soil conditions; and the accident in terms of its explosion characteristics, radiation release, principal pathways, and types of particles released.

13.3.3.1 Location, Climate, and Soil Conditions

The ChNPP exclusion zone is located in the central part of the Ukrainian Polessye physiographic province. The term “exclusion zone” refers to an area surrounding the site that was sealed off as an institutional control to prevent further access after the accident. Immediately after the accident, the exclusion zone was established within the radius of 30 km from the ChNNP. However, as more measurements of the level of contamination over a larger territory were made, the boundary of the exclusion zone was adjusted to prevent access to highly contaminated areas. Its total area within the Ukrainian borders, except for part of the Kiev reservoir, is 2,044 km^2 (Shestopalov 1996 [107844], p. 3).

The Chernobyl region has a humid climate, with mild, short winters and a warm summer. Average annual precipitation ranges from 550 to 750 mm/yr. The relief consists of slightly undulating plains and ridges, and irregularly located bogs. The relatively dense network of Pripyat and Dnieper River tributaries forms boggy valleys of moderate relief. Approximately 50% of the land in the exclusion zone is covered by forest, 30% by arable farm land, and the remaining 20% by urban areas, marshlands, and water bodies (Shestopalov 1996 [107844], p. 22). The soils are relatively homogeneous, with mostly podsols and peaty podsols (soils of forested, temperate climates) as the topsoil layer in the exclusion zone.

13.3.3.2 Type of Explosion and Amount of the Radionuclide Release

The initial explosion at Chernobyl was a steam explosion (Bar'yakhtar et al. 2000 [157504], pp. 12–13; Tarapon 2001 [156920], p. 95). The total amount of radionuclides released by the accident into the environment expressed in becquerels (Bq) was approximately 11×10^{18} Bq (expressed in curies [Ci] this would equal 3×10^{8} Ci), while approximately 6×10^{17} Bq (1.6×10^{7} Ci) of long-lived radionuclides remained in the destroyed reactor. (Note that 1 Ci = 3.7×10^{10} Bq). The kinetic energy released from the accident has been estimated to be equivalent to 30–40 tons of trinitrotoluene (TNT) (Bar'yakhtar et al. 2000 [157504], p. 13). This was the highest single release of radionuclides into the global environment, with contamination calculated to be equivalent to that of a 12 Mt (megaton) nuclear explosion (Bar'yakhtar et al. 1997 [156953], p. 224). No other nuclear accident approaches the dimensions of the Chernobyl disaster in terms of radiological release, acute radiation health effects, and socioeconomic and psychological impact (Bar'yakhtar et al. 2000 [157504], p. 9).

The Chernobyl accident released approximately 2,000 Ci of isotopes of $^{239,\ 240}$Pu into the atmosphere (Bar'yakhtar et al. 2000 [157504], Table 2.5.1; Bondarenko 1998 [156952], p. 13, 15). This amount of radiation is comparable to about 0.5% of the total global fallout of these isotopes from nuclear weapons testing from 1945 to 1963 (Bondarenko 1998 [156952], p. 13; Bondarenko et al. 2000 [156593], p. 473). The activity of plutonium isotopes, distributed outside the 30 km exclusion zone, was 1,344 Ci, or 5×10^{13} Bq. The specific activity of α-emitting isotopes of plutonium was calculated to be 1.5×10^{13} Bq/t (Bondarenko 1998 [156952], p. 23).

13.3.3.3 Principal Pathways

The initial explosion and heat plume at Chernobyl carried volatile radioactive materials up to 1.5 km (0.93 miles) in height, from where these materials were transported over large distances by prevailing winds (Figure 13.3-2). About a quarter of the total released radioactivity entered the atmosphere during the first day after the accident. By the fifth day, the release had decreased approximately sixfold, because of mitigation efforts at the ChNPP. The radionuclides that escaped into the atmosphere then migrated and settled in different areas, causing radioactive contamination of living things. Crops, vegetables, grasses, fruits, milk, dairy products, meat, and eggs were contaminated with radionuclides. The most severe radioactive contamination of fields, rivers, tributaries, canals, drainage ditches, and agricultural lands occurred in the Pripyat and Dnieper river basins that surround the ChNNP.

As part of the cleanup effort after the Chernobyl accident, approximately 8×10^{15} Bq of high-, medium-, and low-level radioactive waste (in mostly solid form, such as construction parts, concrete, and soils) were accumulated and stored at more than 800 interim storage and disposal places in the region (Poyarkov 2000 [157503], pp. 1–2; Kukhar' et al. 2000 [157506]). Infiltration through unlined waste storage and disposal sites has caused leaching of contaminants, so these sites provide the current localized source term for soil and groundwater contamination (Shestopalov and Poyarkov 2000 [157507], pp. 146–147).

Figure 13.3-3 illustrates the principal pathways for radionuclides entering the biosphere through terrestrial and aquatic ecosystems after the Chernobyl accident.

13.3.3.4 Types of Particles Released

Two main types of radioactive particles were released from the damaged reactor: (1) a fuel component of finely dispersed fuel particles, containing elements of low volatility, such as cerium, zirconium, barium, lanthanum, strontium, and the actinides; and (2) a condensed component that formed when gases of nuclides (such as iodine, tellurium, cesium, and a lesser amount of strontium and ruthenium) that were ejected during the nuclear fuel fire, condensed on different surfaces (e.g., ground, buildings, and trees–Kashparov 2001 [156819], pp. 11–12). Fuel particles settled primarily on the land surface near the ChNNP zone (Kashparov 2001 [156819], pp. 24, 26).

Hot particles formed from both fuel and condensed components, including particles of uranium dioxide (a few tens of μm in diameter or smaller) made of fuel fused with the metal cladding of the fuel rods and fuel mixed with sand or concrete (Loshchilov et al. 1991 [125894]; NEA 1995 [156632], p. 53). Hot particles have an activity concentration exceeding 10^5 Bq/g (Bar'yakhtar 1997 [156953], p. 235). Chernobyl hot particles behaved differently from nuclear bomb particles and Chernobyl gaseous and aerosol forms (Zheltonozhsky et al. 2001 [156630], p. 151). For example, Chernobyl hot particles (1) did not contain activation products such as ^{60}Co; (2) contained ^{125}Sb and ^{144}Ce, which are absent in atomic bomb hot particles; (3) contained a larger fraction of ^{137}Cs than that in nuclear bombs; (4) had a ratio of ^{154}Eu/^{155}Eu about 10 times greater than that in atomic bomb particles and about 200 times than that in fusion bomb particles; (5) have a lower radiation of uranium and neptinium than that from fusion bombs; and (6) had a lower plutonium content than that in the fusion bombs (Zheltonozhsky et al. 2001 [156630], pp. 156–159). After nuclear weapons testing, over 90% of the activity of ^{90}Sr and ^{137}Cs was present in water-soluble and exchangeable forms in global fallout, but after the Chernobyl accident, the fraction of exchangeable forms of ^{90}Sr and ^{137}Cs in the near-ChNNP zone in 1986 was less than 25% of their activity in a fallout, and the remaining activity was caused by nonexchangeable forms of these radionuclides associated with fuel particles (Kashparov 2001 [156819], p. 27). ^{90}Sr, ^{106}Ru, ^{134}Cs, ^{137}Cs, ^{144}Ce, and ^{147}Pm contributed to the total β-activity of hot particles (Papp et al. 1997 [124806], p. 951). Isotopes of actinide elements ^{238}Pu, ^{239}Pu, ^{240}Pu, and ^{242}Cm contributed mostly to the total α-activity of hot particles. The surface density of hot particles was about 1,600 per m^2 in downtown Kiev (Papp et al. 1997 [124806], p. 951). Hot particles were detected not only on the surface, but they also migrated in soils to depths of about 0.5 m (Gudzenko 1992 [107835], p. 2), as detected in the fall of 1987 (Gudzenko et al. 1990 [125020], p. 122).

The released fuel particles that entered the atmosphere are categorized by relative size into large (tens to several hundred μm) and small particles (median radius of 1.5–3.5 μm). The large fuel particles were formed from the fragmentation of the fuel at high temperatures during the initial phase of the accident. The large particles were primarily deposited within a 5 km zone around the damaged reactor. Small fuel particles consisted of unoxidized uranium dioxide (Bar'yakhtar et al. 2000 [157504], pp. 21–22). Note that hot particles <10 μm in size can be inhaled into the lungs (Loshchilov et al. 1991 [125894], p. 47).

13.3.4 Soil Contamination

This section provides an overview of the distribution of soil contamination resulting from the Chernobyl accident and characteristics of actinide element migration in soils.

13.3.4.1 Lateral Distribution of Soil Contamination

The prevailing wind directions and velocities that occurred immediately after the Chernobyl accident established the contaminant fallout trajectories (see Figure 13.3-2). The surface deposition of contaminants is affected mainly by local wind patterns and rain conditions existing at the time of the accident. Therefore, the surface contamination resulting from the Chernobyl accident is extremely irregular over very large areas. The contaminated spots range in size from a few square meters to more than a thousand square kilometers (Shestopalov 1996 [107844], p. 14). The data on air transport of contaminants demonstrate the important role of the local spatial and temporal patterns in the wind direction and the need for estimating both the source strength and the lateral distribution of contaminants in numerical models (Goldman et al. 1987 [156820]). The area of highest concentration of ^{137}Cs is the "Western finger," which extends almost in a straight line westward from the ChNPP. The plume is 1.5 to 5 km wide; for a distance of <70 km the concentration of ^{137}Cs along its axis decreases from >10,000 Ci/km^2 (3.7×10^5 kBq/m^2) to 10 Ci/km^2 (3.7×10^2 kBq/m^2). Because of the local wind pattern, the "Southern finger" splits into five separate tracks and has the highest concentrations of ^{90}Sr and actinides. The pattern of the widespread "Northern finger" was likely formed by deposition with rain. The "South-West finger" has the most complex, vortex-like shape (Shestopalov 1996 [107844], pp. 13–14).

The results of large-scale soil sampling on a regular grid of about 1 km (radius of 36 km) are shown on two maps of ^{90}Sr and ^{137}Cs contamination in Figure 13.3-4. The difference in distribution patterns for ^{90}Sr and ^{137}Cs is caused by different processes of precipitation for these radionuclides: ^{90}Sr was ejected with fuel particles and precipitated mainly in the near ChNNP zone, while ^{137}Cs was contained in the condensed component, which moved and precipitated further away from the ChNPP (Kashparov 2001 [156819], pp. 24–26). These maps were used to estimate the total contents of radionuclides on the ground surface of the 30 km exclusion zone (without the reactor site and the radioactive waste disposal sites), which showed that initial estimates of the contamination were overestimated. For example, the content of ^{90}Sr is estimated to be approximately 810 TBq (8.1×10^{14} Bq) for the Ukrainian territory, which is 3 to 4 times lower than previous estimates (Kashparov et al. 2001 [157400], p. 295).

13.3.4.2 Vertical Distribution of Radionuclides in Soils

Silant'ev et al. (1989 [126508], p. 224), Isaksson and Erlandsson (1998 [156617], p. 150), and Likar et al. (2001 [156627], Figure 2) determined that, overall, the concentration of radionuclides in the soil profile decreases exponentially with depth to a depth of approximately 3 cm. In the exclusion zone, the downward velocity of migration of ^{137}Cs ranged from 0.4 to 0.7 cm/yr in the first years after the accident, and then dropped to 0.2 cm/yr (Bar'yakhtar 1997 [156953], p. 247).

Vertical migration of uranium and plutonium in soils is limited to the topsoil layer, because these radionuclides were released as hot particles that are more or less stable in the near-surface weathered zone. Table 13.3-1 shows that about 99% of plutonium accumulated within the top 2

cm soil layer. This table also shows that the $^{238}U/^{235}U$ ratio remained unchanged below a depth of 3 cm. Figure 13.3-5 shows measurable quantities of actinides (plutonium, americium and curium) in soil to a depth of 4.5 cm, in spring 1994, in the Kopachi village, located a few kilometers from the ChNNP (Mboulou et al. 1998 [156628]). Figure 13.3-6 shows the actual and predicted distribution of activities with depth for ^{90}Sr, ^{137}Cs, and ^{239}Pu. The total activity of all these radionuclides is mostly in the upper 3 cm layer.

Radionuclide releases from hot particles present an additional source of soil contamination, causing the concentration of mobile ^{137}Cs in soils to reach a maximum 1.5 to 2.5 years after the accident and concentration of ^{90}Sr to reach a maximum 6 to 15 years after the accident (Bar'yakhtar 1997 [156953], p. 243). The decrease in ^{137}Cs concentration in soils in the exclusion zone by about 25%–50%, as observed 10 years after the accident, was caused by several factors (Shestopalov 1996 [107844], p. 14): (1) natural radioactive decay of ^{137}Cs (about 20%); (2) partial washout of the soil surface layer from elevated areas and slopes; (3) soil decontamination; and (4) migration deeper than 20 cm from the soil surface along the zones of preferential flow. A secondary contamination by ^{137}Cs affected many areas, such as local soil depressions, edges of marshes, and reservoir banks, where ^{137}Cs concentration increased by a factor of 2 to 10, and locally up to 50 to 250 times. Concentration of ^{137}Cs in the exclusion zone reached 50,000 to 150,000 Ci/km^2, which is 5 to 15 times greater than that in soils in the so-called “Red Forest” around the ChNPP, where intense radioactivity caused leaves to lose chlorophyll and turn red.

13.3.4.3 Characteristics of Migration of Actinides in Soils

Within the European part of the former Soviet Union, the plutonium content in soils after the Chernobyl accident varies from 10 to 3,700 Bq/m^2 (Lebedev et al. 1992 [125854], p. 516). The typical content of $^{239,\,240}Pu$ in Ukraine soils is 70 Bq/m^2 (Bondarenko et al. 2000 [156593], p. 473). The determination of the isotopic composition of plutonium, and especially the ratio $^{238}Pu/^{239,\,240}Pu$, is important to assess the source of soil contamination. For example, for the global fallout, this ratio is typically from 0.03 to 0.05. However, in Chernobyl soil samples, this ratio varied from 0.25 to 0.35, which corresponds to the ratio of about 0.3 in spent fuel (Lebedev et al. 1992 [125854], p. 517). In contrast to the radioactive gases and relatively mobile radionuclides such as iodine and cesium, isotopes of plutonium, americium, and other actinides are associated with fuel particles.

Bondarenko (1998 [156952]) and Bondarenko et al. (2000 [156593]) presented the results of an 11-year investigation (1986–98) of the migration of long-lived α-emitting transuranic (TRU) elements in ecologic chains and the human body. The accumulation of TRU elements in plants showed significant variability, depending on the type of soil, vegetation, and presence of microbial activity. The ratio of concentrations of TRU elements in plants varies within several orders of magnitude among the isotopes of each element. The main pathways for the entrance of TRU elements in the human body are ingestion of food and water, and inhalation (Bondarenko 1998 [156952], Section 5; Bondarenko et al. 2000 [156593], pp. 473–474). Migration of TRU elements that accumulated in hot particles begins as hot particles are broken down.

Thus, near-surface soil contamination by ^{90}Sr, ^{137}C, and TRU elements is widespread within a large area around Chernobyl, but vertical distribution of contaminants is mostly limited to depths of several centimeters. This creates favorable conditions for the atmospheric resuspension and

secondary deposition, as described in Section 13.3.5, of hot particles and radionuclides attached to soil particles as a result of wind erosion.

13.3.4.4 Technetium in Soils

At present, there are only limited data on concentration of ^{99}Tc in the environment caused by the ChNPP accident. Uchida et al. (1999 [156945]; 1999 [156925]) presented results of ^{99}Tc measurements in soil samples collected within three forest sites around Chernobyl in 1994 and 1995. Two sites were located 28.5 km and 26 km to the south, and one site is 6 km to the southeast of the ChNPP. The ^{99}Tc concentration was determined by inductively coupled plasma mass spectrometry after its chemical separation from the soil sample. Concentrations of ^{99}Tc in these soil samples ranged from 1.1 to 14.1 Bq/kg at a depth of 6–9 cm, which is one to two orders of magnitude higher than those under background conditions. The regression function describing the change of the ^{99}Tc concentration with distance is ^{99}Tc concentration = $4.88 \times R^{-1.771}$, where ^{99}Tc concentration on the ground is in GBq/km^2 (Note: 1 GBq = 10^9 Bq) and the distance R is in kilometers from the ChNPP (Uchida et al. 1999 [156925], p. 2,764).

The most stable form of technetium under aerobic conditions is Tc(VII), TcO_4^-, which is characterized by high mobility in soils and availability to plants. Under anaerobic conditions and increased soil-water saturation (for example, under irrigation), TcO_4^- could be transformed to a lower oxidation state of Tc(IV), to Tc sulfide forms, or to organic bound forms, which are insoluble and will adsorb and accumulate in soils with time (Tagami and Uchida 1999 [156923], pp. 963-964).

13.3.5 Erosion and Atmospheric Resuspension of Radionuclides

After the Chernobyl release ended, atmospheric resuspension of radionuclides became a secondary source of contamination, which affected people in areas that were not exposed to the original release (Garger et al. 1996 [156602], p. 18). The main cause for the resuspension of radionuclides is wind erosion of soil. The average annual soil erosion in Ukraine from 1987 to 1990 due to spring winds was 1 t/ha (tons/hectare) (Prister et al. 1991 [156824], p. 74), which, for topsoil with a density of 1.3 g/cm^3, corresponds to soil loss of 8×10^{-3} cm/year. Erosion led to the total (spring and fall) annual removal of 0.7×10^5 Bq/ha of ^{137}Cs from soils, with a concentration activity of 1×10^3 Bq/kg (Prister et al. 1991 [156824], Table 7).

Resuspension of radionuclides with dust driven by wind is especially hazardous in agricultural areas. The resuspension of particles with ^{137}Cs increases after the tillage of agricultural lands from background conditions of 0.7 Bq (m^2/day) to 10 Bq (m^2/day) (Loshchilov et al. 1991 [156828], p. 64). For rural areas in Ukraine with different agricultural activities, the concentration of dust in air ranged from 0.3–203 mg/m^3 for a soil moisture content of 3–20% (Loshchilov et al. 1991 [156823], p. 199, Table 1). The maximum concentration of dust in samples collected from air stirred up by agricultural machinery in the Ukraine was 4,000 mg/m^3 during potato planting (Anokhova and Krivtsov 1991 [156829], p. 206).

In the topsoil layer, radionuclides are attached mostly to small soil particles that are less than 1 μm in diameter (Loshchilov et al. 1991 [156823], p. 198). Therefore, the specific activity of small soil particles exceeds that for largest particles (0.1–1 mm; Anokhova and Krivtsov 1991

[156829], p. 206). For example, for ^{134}Cs the specific activity of small particles exceeds that of large particles by a factor of 12.7, for ^{137}Cs by a factor of 9.1, for ^{90}Sr by a factor of 7.4, and for $^{238+239+240}Pu$ by a factor of 19.2 (Anokhova and Krivtsov 1991 [156829], Table 2, p. 208). The specific radioactivity of resuspended dust particles (<10 μm) increases by a factor of 10 compared to that in soils, from which these particles were originated (Loshchilov et al. 1991 [156823], p. 200).

One of the main parameters characterizing the atmospheric resuspension of radionuclides is the resuspension factor. The resuspension factor is defined as the ratio between the airborne (Bq/m^3) and surface (i.e., <1 cm depth) concentration (Bq/m^2) of a radionuclide in question. According to Bondarenko et al. (2000 [156593], pp. 474–475), the resuspension factor in 1998 ranged from 0.34×10^{-10}–17×10^{-10}/m. This value is in agreement with the range of resuspension factors (from 1.4×10^{-10}/m for ^{137}Cs and 1×10^{-11}/m for $^{239,240}Pu$) determined in 1998 by Rosner and Winkler (2001 [156629], pp. 11, 17). The resuspension factor was higher at the earlier stage after the accident. For comparison, in the Yucca Mountain Biosphere Process Model, the resuspension-factor mean value is 8.3×10^{-11}/m (CRWMS M&O 2000 [151615], Section 3.2.4.1.3).

Kashparov et al. (2000 [156622]) investigated the resuspension and redistribution of radionuclides at various distances from fires occurring in areas previously contaminated by the Chernobyl accident and outside the 30 km ChNPP exclusion zone. They determined that the resuspension factor for the active phase of a fire was as high as 10^{-7}–10^{-8}/m (Kashparov et al. 2000 [156622], p. 288). The dose coefficient from the radioactive aerosol inhalation was estimated to be 1.5×10^{-8} Sv (1 Sv = 100 rem), which provides less than 1% of the total dose resulting from inhalation and external radiation (Kashparov et al. 2000 [156622], p. 296). This value for the dose coefficient was obtained for a one-year period following a single intake of radionuclides due to a fire (Kashparov et al. 2000 [156622], p. 297). Equivalent dose is the quantity obtained by multiplying the absorbed dose (the quantity of energy imparted by radiation to a unit mass of matter such as tissue, measured in SI (International System of Units) units in grays, Gy, or rad) in a body organ or tissue by a factor representing the effectiveness of the type of radiation causing harm to the organ or tissue (NEA 1995 [156632], p. 60). Effective dose is the weighted sum of the equivalent doses to the various organs and tissues, multiplied by weighting factors reflecting the differing sensitivities of organs and tissues to radiation (NEA 1995 [156632], p. 59). In SI units, equivalent dose is measured in sieverts (Sv). The whole-body (internal and external) dose (i.e., total effective dose equivalent [TEDE]) limit for a radiological worker is 5 rem/year (DOE 1994 [104736], p. 2-6, Table 2-1). The presence of α-emitting radionuclides (in the 30 km zone) causes a considerable increase in inhalation dose during forest fires, which can exceed external exposure doses (Kashparov et al. 2000 [156622], p. 297).

Thus, measurements and modeling investigations indicated that radionuclide resuspension could become a source of both external and inhalation radiation doses for people, depending on the distance from the release. The size distribution of resuspended particles is important in determining inhalation (i.e., lung) dose.

13.3.6 Groundwater Contamination

This section examines the extent of groundwater contamination resulting from the Chernobyl accident and the type of radionuclides involved.

The largest source of radionuclide contamination of groundwater is from about 800 radioactive waste disposal sites within the Chernobyl exclusion zone. Another large, local source of contamination is the Chernobyl cooling pond (Shestopalov and Poyarkov 2000 [157507], p. 146). Radionuclides dispersed over large areas can migrate to the water table through and around casings of boreholes and in colloidal and dissolved states in percolating water from the vadose zone. Field investigations showed a lack of correlation between ^{137}Cs soil concentration and its travel time to the water table (Gudzenko et al. 1991 [107834], p. 3), indicating that soil contamination is not a major source of groundwater contamination.

Before the Chernobyl accident, the depth to the water table around the ChNPP was approximately 6 to 8 m and was controlled by several drainage systems. Since 1986, some drainage systems have been abandoned, so that the water table has risen, creating a potential instability for the remaining structure of the ChNPP. Subsequently, several countermeasures, such as the construction of a vertical drainage system and an impermeable underground vertical wall, allowed the water table to decline to previous depths.

The highest ^{90}Sr concentrations of groundwaters (10^2–10^4 Bq/L) were measured in water samples taken at interim radioactive storage sites near the ChNPP (Table 13.3-2). By 1995–1996, an increase in the ^{90}Sr and ^{137}Cs concentrations by 2–3 orders of magnitude, in comparison with pre-accident conditions, occurred in the upper section of groundwater within the inner part (5–10 km) of the exclusion zone. At the same time, radionuclide concentration in the groundwater and the artesian aquifer are below the maximum permissible concentration. Despite a low level of current contamination of the artesian aquifer in the Eocene deposits, which is the source of potable water within the exclusion zone, it is predicted that groundwater contamination will increase over the next few decades (Shestopalov and Poyarkov 2000 [157507], p. 141).

The presence of ^{134}Cs in groundwater and the increase of ^{90}Sr concentration by two orders of magnitude (from 4–400 mBq/L) confirm that radionuclides from Chernobyl reached groundwater at 50 to 70 m depths over five years (1987-1992) (Bar'yakhtar 1997 [156953], p. 254). Cs-137 and ^{90}Sr contamination was detected in the Cretaceous aquifer at depths of 80 to 120 m within the 30 km zone 22 months after the accident (Gudzenko 1992 [107835], p. 5). Elevated concentrations of ^{90}Sr and ^{137}Cs occurred at substantial distances from the ChNPP plant in all aquifers down to 200–300 m (Table 13.3-3).

Given these findings, groundwater contamination by ^{90}Sr and ^{137}Cs, caused by leakage from radioactive waste disposal sites within the Chernobyl exclusion zone, cooling pond, and migration through casings of boreholes to depths below 120 m, is expected to influence all nearby aquifers. However, the risk associated with the use of contaminated groundwater water for water supply is marginal, as compared to external radiation and inhalation doses (see Sections 13.3.7 and 13.3.9).

13.3.7 Using Contaminated Water for Irrigation and Water Supply

The Dnieper River water is used for irrigation of more than 1.8 million hectares in Ukraine, involving the territories from Kiev in the north to Crimea in the south (Berkovski et al. 1996 [156592], p. 39). Figure 13.3-8 shows the concentration of radionuclides in water from six reservoirs along the Dnieper River used for irrigation. In the southern Ukraine, which has a semi-arid climate and a depth to the water table of 50–70 m, irrigation water is taken mostly from canals extending from the Dnieper River reservoirs. About 50% of the land is used to plant fodder crops, eventually leading to the contamination of meat and milk products, and about 10% is used to plant vegetables (Berkovski et al. 1996 [156592], p. 39). The water loss into the subsurface on irrigated lands and from irrigation canals accelerates migration of the radioactive elements from crops, soil surface, and surface water sources into the vadose zone and groundwater. The amount of radionuclides migrating into the subsurface depends on the quality (pH and chemical composition) of the irrigation water and soils, soil structure, depth to water table, and evapotranspiration, as well as the type of irrigation.

Table 13.3-4 illustrates that the concentrations of ^{137}Cs in grains, grass, and vegetables grown on lands that were irrigated with contaminated Dnieper River water exceeded by a factor of 2–6 those in crops irrigated using uncontaminated water, while the concentrations in irrigation water increased by a factor of 2–4 (Perepelyatnikov et al. 1991 [156822], p. 112, Table 5). The increase in the concentration observed during irrigation confirms the concept of a buildup factor in soils.

Table 13.3-5 indicates that the accumulation of radionuclides on irrigated lands occurred to depths of at least 10–20 cm. An example is data on the distribution of ^{137}Cs and ^{90}Sr in soils irrigated using contaminated water in the southern Ukraine (Perepelyatnikov et al. 1991 [156822]). After the rice harvest in 1988, irrigation caused an increase in the ^{137}Cs concentration in the 0–0.5 cm topsoil layer by 58% compared to that on unirrigated (bare) lands. In the 0.5–2 cm layer, its concentration increased by 14–19%. For the same time period, the ^{90}Sr contamination increased by a factor of ~2 (from 18–35 mCi/km^2) in comparison with that of bare soil (i.e., without vegetation and irrigation). The accumulation of ^{137}Cs and ^{90}Sr in soils caused the concentration of these radionuclides in rice to increase. For example, in the first harvest after the accident in 1986, the ^{137}Cs concentration increased by a factor of 1.6 compared to 1985 concentrations. The ^{90}Sr concentration began to increase in 1987, and it increased by a factor of 1.3 compared with 1985 values. However, in the southern Ukraine, concentrations had not reached levels detected in 1972, from global fallout generated by nuclear testing (Perepelyatnikov et al. 1991 [156822], pp. 110, 112, Table 4).

Using the average concentrations of ^{137}Cs and ^{90}Sr in the 20 cm soil layer obtained after three years of rice irrigation (last column of Table 13.3-5) and concentrations in bare soils (third column of Table 13.3-5) assuming that the preaccident concentration is equal to that of bare soils, the following buildup factors are obtained: for ^{137}Cs, 0.48/0.37 = 1.3 (for three years), or approximately 10% per year; and for ^{90}Sr, 116/60 = 1.97 (for three years), or approximately 32% per year. It is expected that the radionuclide buildup factor in soils under irrigation will change with time, depending on the processes of leaching and ecological decay of radionuclides.

Thus, irrigation with contaminated water in the southern Ukraine leads to the accumulation of radionuclides in both the topsoil layer and in crops. The data obtained in Ukraine qualitatively confirm the concept of a radionuclide buildup factor in irrigated soils; this concept is employed in the Yucca Mountain Biosphere Process Model.

13.3.8 Leaching and Transfer Coefficients

This section discusses the dissolution rate, leaching parameters, soil-plant transfer of radionuclides, and radionuclide accumulation in fish and livestock.

13.3.8.1 Dissolution Rate and Leaching Parameters

Hot particles exposed at the surface were oxidized, which caused superficial cracking of the particles and increased their surface area, which in turn led to higher dissolution rates. The dissolution rates for nonoxidized and oxidized fuel particles (UO_{2+x}) differ with acidity of the solution (Kashparov et al. 2000 [156623], p. 232). The dissolution rate V for fuel particles depends on the soil pH according to the formula (Bar'yakhtar et al. 2000 [157504], p. 32):

$$V = a \times 10^{b\,\mathrm{pH}}\ \mu\mathrm{m/yr} \qquad \text{(Eq. 13-1)}$$

where coefficients a = 14.45 and b = –0.431 for weakly oxidized particles, and a = 4.59 and b = -0.234 for strongly oxidized fuel particles. This formula was used to describe radionuclide leaching from fuel particles for pH from 4 to 6. Kashparov et al. (2000 [156623], p. 232, Figure 4), who studied dissolution kinetics of Chernobyl fuel particles over a pH range from 3 to 9, determined that the dissolution rate is minimal in a neutral medium, while it increases in both acidic and alkaline media.

A study of concentrations of Chernobyl radionuclides in Neuherberg, Germany, was carried out by Rosner and Winkler (2001 [156629]). They determined that the annual mean concentrations in air and annual deposition to ground decreased for ^{90}Sr, ^{137}Cs, ^{238}Pu, and ^{239,240}Pu from July 1986 to 1998. Figure 13.3-9 shows annual mean values of radionuclide concentrations in air (μBq/m^3), specific activities in air dust (Bq/g), and radionuclide ratios in air (Bq/Bq) at Munich-Neuherberg since 1985. The air-dust concentration (μg/m^3) is shown in this figure for comparison.

The leaching coefficient is defined as a parameter characterizing the downward movement of radionuclides dissolved in percolating waters (CRWMS M&O 2001 [152517], p. 6) and is calculated as part of the total mass of the radionuclide leached from a soil layer per unit of time (CRWMS M&O 2001 [152517], Section 5.1, Equation 1).

The leaching coefficient for ^{90}Sr determined using Chernobyl data varies significantly from 3×10^{-2}–3.1 L/yr (Bar'yakhtar 1997 [156953], p. 240). For comparison, the leaching coefficient for ^{90}Sr used in the Yucca Mountain biosphere process model is 4.47×10^{-2} L/yr (CRWMS M&O 2000 [151615], Table 3-7), which is near the lower limit of the Chernobyl range. The dissolution rate of uranium reached 2.2×10^{-2} L/yr using Chernobyl data (Bar'yakhtar 1997 [156953], p. 241).

The release of radionuclides from solid particles into the soil is governed by the diffusion process (Sobotovich and Dolin 1994 [156821], p. 57). Given the diffusion coefficients for ^{90}Sr ($1.3–2.1 \times 10^{-16}$ cm^2/s) and ^{137}Cs ($2.5–4.8 \times 10^{-17} cm^2/s$), about 65–80% of ^{90}Sr will become mobile in 10 years, and only 20–30% of ^{137}Cs will become mobile over the same time (Sobotovich and Dolin 1994 [156821], p. 59, 60).

Smith et al. (2000 [156906], p. 141) hypothesized that the "fixation" process of radionuclides controls the amount of cesium in soil water and therefore its availability to terrestrial biota. The decline in ^{137}Cs mobility and bioavailability over the first few years after fallout is most likely controlled by slow diffusion of ^{137}Cs into the soil's illitic clay mineral lattice. However, the sorption-desorption process may be reversible for ^{137}Cs, in which case the ecological half-life increases towards its physical half-life decay rate of 30.2 years. Smith et al. (2000 [156906], p. 141) showed a two-component exponential decline model for the ^{137}Cs decline in vegetation, water, and fish.

13.3.8.2 Soil-Plant-Food Transfer of Radionuclides and Food Contamination

Two main mechanisms control radionuclide transfer to plants: (1) direct deposition on plant surfaces from atmospheric resuspension of contaminated soil and from irrigation with contaminated water, and (2) the root uptake of radionuclides. For example, immediately after the Chernobyl accident, when aerosol particles accumulated only on the outer bark of trees, the radioactivity of leaves of some trees in the streets of central Kiev in 1986 varied from 70,000–400,000 Bq/kg (Bar'yakhtar 1997 [156953], pp. 260, 261). At that time, inner tissues of trees and roots did not pick up contamination. Radioactivity of the outer bark of trees decreased in 5–6 years after the accident, while the activity in wood and inner bark increased because contaminants migrated through the root systems. According to Prister et al. (1991 [157548], p. 146) root uptake became significant the second year after the accident. Bulgakov and Konoplev (2000 [156699], p. 776), who reviewed the existing information on root uptake and modeled root uptake by pine trees within the Chernobyl exclusion zone, stated that the radionuclide concentration at the bottom of the root system is the same as in the most contaminated part of the topsoil layer, and the radiocesium transfer from the root's exchangeable complex into the above-surface part of the plant is relatively rapid. For grass, this takes one day. Radionuclide migration from roots into tree trunks is limited by diffusion and convective radionuclide transfer from the soil into the roots.

The soil-to-plant transfer factor (or concentration ratio) is defined as the ratio of radioactivity concentration in the edible part of the plant (Bq/kg) to the radioactivity concentration in soil (Bq/kg). This factor is also termed the accumulation factor by Bar'yakhtar (1997 [156953], p. 270). Table 13.3-6 compares the soil-to-plant-transfer factors for different radionuclides in the Yucca Mountain Biosphere Process Model with those in Chernobyl. The range of these factors for each element depends on many processes affected by the type of elements and soil properties, plant species, concentration of nutrients and carrier elements in soils, moisture content, acidity of soils, and meteorological and climatic conditions.

The soil-plant transfer processes are not important for short-lived radionuclides, such as ^{131}I, because they essentially decay before being taken up by plant roots. The transfer of radionuclides from soils to plants is limited to long-lived radionuclides. However, the soil-plant transfer is a

predominant pathway for cesium and strontium to appear in pasture and/or fodder, and subsequently in meat and milk, thus becoming part of the exposure pathway. Table 13.3-7 summarizes the values of the cesium soil-to-fodder transfer coefficients, depending on the soil pH and types of agricultural products. This table shows that transfer factors for ^{137}Cs vary significantly (several orders of magnitude) depending on types of soils and plants, because of the effects of microbiological activity in soils (metabolism and decay of microorganisms), and in the presence of different complex-forming ligands (Bondarenko 1998 [156952], pp. 28–31).

A plausible explanation for the observation in Table 13.3-7 that transfer coefficients are higher in natural grasses than in other fodder types could be the following. The transfer coefficients depend on the diffusion of radionuclides into the root system. Natural grasses grow on undisturbed soils with better contact between the soils and roots, which increases the diffusion of radionuclides into grasses. In contrast to undisturbed soils, cultivated soils do not have as good contact with the roots, which reduces diffusion of radionuclides into the plants. At the same time, cultivated soils experience more significant weathering and resuspension of radionuclides by wind. Furthermore, application of fertilizers to cultivated soils and soil-plant microbiological activity may immobilize radionuclides.

The effective meadow-vegetation transfer coefficient for ^{90}Sr is of the same order of magnitude as in alfalfa, and is shown in Figure 13.3-10. Accumulation of ^{137}Cs in vegetables (cucumber and tomato) is higher than in wheat and corn (see Table 13.3-4). Accumulation of ^{137}Cs in some meadow grasses depends on the type of soils and increases in wet soils (Shestopalov and Poyarkov 2000 [157507], Table 5.6.3). The data given in this figure can be used to estimate that the transfer coefficient for ^{90}Sr increased from 1×10^{-3}–1×10^{-2} m^2/kg from 1988 to 1994. This increase can be explained by the fact that ^{90}Sr, which settled on soils, is gradually transformed into a soluble form and thus absorbed by plants.

Bruk et al. (1998 [156600], p. 178) determined that during the first five to six years after deposition, the ^{137}Cs concentration in vegetables and animal agricultural products decreased with an environmental half-life period of 0.7–1.5 years (i.e., the length of time required for ½ of the radioacting to decay *in situ*). Thereafter, beginning from 1990–1991, no significant variation of the ^{137}Cs content in food products was found, and the values of the transfer factors for this radionuclide in the main types of food (milk, potatoes) for rural inhabitants were close to those obtained in the pre-accident period (1980–1985), based on the global origin. Reduction of the ^{137}Cs content in produce was most rapid during the early years after the accident, as intensive countermeasures were applied at that time. Half-life periods for ^{137}Cs content in milk (the basic dose-forming product) and other products for the most contaminated areas in Russia amounted to 1.6–4.8 years, depending on the type of countermeasures used. Half-life periods of the decrease in the ^{137}Cs content in other types of agricultural products (grain, potato) were within the range of 2–7 years. Ivanov (2001 [156818], pp. 65–66) approximated the dynamics of the transfer coefficient for ^{137}Cs in the chain soil-plant by a function

$$y = a \exp(-bt) + (1-a) \exp(-ct) \qquad \text{(Eq. 13-2)}$$

where y is the transfer coefficient normalized to the maximum transfer coefficient, t is the time (in years), and a, b, and c are parameters that depend on the type of soil and plants: a = 0.76–0.94, b = 0.44–1.38, and c = 0.038–0.17 (Ivanov 2001 [156818], p. 67, Table 5). According to

Ivanov (2001 [156818], Table 6), the ecological half-life of ^{137}Cs in agricultural plants varied in terms of averaged values from 0.42 (first period) to 22.1 (second period) years, depending on the type of soils. Figure 13.3-11 presents the dynamics of the transfer coefficient for ^{137}Cs in meadow grass.

Zhdanaova et al. (2000 [156951], p. 64) determined that interaction between biota and *micromycetes* fungi destroyed hot particles after the Chernobyl accident. They determined two mechanisms responsible for these processes: (1) microbial metabolic activity; and (2) mechanical destruction by mycelial overgrowth of radioactive particles. From this, it follows that these processes may also decrease the half-life of radionuclides in the environment, compared with physical half-life values. Therefore, the use of physical values of the half-life of radionuclides gives conservative estimates of radionuclide migration in the Yucca Mountain Biosphere Process Model.

Based on an extensive experimental and modeling study of transfer factors for mushrooms, wild animals, berries, meat, and milk in different regions of Ukraine, Belarus, and Russia, Jacob and Prohl (1995 [156864], p. 110) determined that a peroral (oral) dose is higher than that from the external radiation. They applied several models in calculating transfer coefficients in the chain soil→plants→food→human body. The soil-milk transfer coefficient ranges from less than 1 to 20 Bq/L per kBq/m^2.

Table 13.3-8 presents concentrations of ^{137}Cs in the pasture, milk and meat, and their daily uptake (Richards and Hance 1996 [157613]). These concentrations are used to calculate transfer coefficients using the following formula (CRWMS M&O 2000 [152435], Table 1)

$$\text{Transfer coefficient} = \text{Concentration in meat or milk} / \text{Intake}$$

For Chernobyl, the meat and milk transfer coefficients are 1.6–2.0 × 10^{-2} day/kg and 6.4–8.0 × 10^{-3} day/L, respectively. For the Yucca Mountain Biosphere Process Model, the beef and milk transfer coefficients are 5 × 10^{-2} day/kg and 8 × 10^{-3} day/L, respectively (CRWMS M&O [151615], Table 3-14). Thus, the Yucca Mountain meat transfer coefficient exceeds that determined for Chernobyl, and the Yucca Mountain milk transfer coefficient is essentially the same as that for Chernobyl.

13.3.8.3 Radionuclide Accumulation in Fish

Smith et al. (2000 [156906]) measured ^{137}Cs activity concentrations in terrestrial vegetation at seven sites, in lake water, and in mature fish in Cumbria, UK. They determined that ^{137}Cs from the 1986 Chernobyl accident has persisted in freshwater fish for much longer than was initially expected because of the so-called “fixation” process of cesium in soil. They concluded that the effective ecological half-life in young fish, water, and terrestrial vegetation has increased from values of 1–4 years measured during the first five years after Chernobyl to 6–30 years determined since 1990. Jonsson et al. (1999 [156620]) measured cesium in nearly 4,000 fish, taking samples 2–4 times every year in a Scandinavian lake contaminated by Chernobyl fallout. The estimated half-life of cesium concentration in fish was 0.3–4.6 years. Jonsson et al. (1999 [156620]) found that the decline in cesium was initially rapid for three to four years and then became much slower. About 10% of the initial peak radioactivity declined with a half-life of 8–

22 years. Smith et al. (2000 [157433]) determined the bioaccumulation factor of different fish in ten lakes of Belarus, Russia, and Ukraine from 1–232 km from Chernobyl from 6–11 years after the accident. They determined that the bioaccumulation factor for ^{137}Cs ranged from 82–14,424 L/kg for different lakes and types of fish (Smith et al. 2000 [157433], Table 2). The bioaccumulation factor used in the Yucca Mountain Biosphere Process Model for freshwater fish for ^{137}Cs is 2,000 L/kg (CRWMS M&O 2000 [151615], Table 3-15), which is within this range. The Yucca Mountain recommendation for the bounding value of the bioaccumulation factor is 15,000 L/kg (CRWMS M&O 2000 [152435], Table 14), which agrees with the maximum value determined by Smith et al. (2000 [157433], Table 2). Smith et al. (2000 [157433], p. 360) used the term *concentration factor*, which is the same as the bioaccumulation factor for the Yucca Mountain Biosphere Process Model.

13.3.8.4 Livestock Uptake

Livestock uptake represents radionuclide transfer to animal food products. The ^{137}Cs transfer coefficients to cattle, milk, and meat in Ukraine from 1987–1993 are different for soils with different soil pH values (Bar'yakhtar 1997 [156953], Table I.5.4). In 1993, radionuclide concentration in beef from collective farms, where fodder was produced on arable soils, ranged from 20–71 Bq/kg. At the same time, the radionuclide concentration in meat from private farms ranged from 75–520 Bq/kg, and in wild animal meat, it ranged from 504–1,540 Bq/kg (Bar'yakhtar 1997 [156953], pp. 370–371). In the Rivne region of Ukraine, the transfer factor for beef ranged from 0.16–0.59 m^2/kg for collective farms, and ranged from 1–1.7 m^2/kg for private farms. The difference between the collective and private farms can be explained by the fact that countermeasures were undertaken on collective farms.

Empirical data from the leaching and transfer coefficients summarized in Section 13.2.8 show that the initial dissolution of hot particles exposed to the atmosphere increases the concentration of radionuclides, which then decreases with time. The ecological half-life of radionuclides in soils, plants, and foodstuff is less than physical values for radionuclides. Diffusion and absorption processes are limiting factors for radionuclide transfer in soils. Radionuclide transfer to a plant depends on two main mechanisms: (1) direct deposition on the plant surfaces from resuspension of contaminated soil particles or from irrigation with contaminated water, and (2) the root uptake of radionuclides, which is limited by diffusion and convective transport from the soil to the root.

13.3.9 Human Receptor Exposure

This section defines the Chernobyl human receptors and critical groups, gives examples of human exposure pathways and BDCF calculations, and presents the radiation doses from plutonium.

13.3.9.1 Chernobyl Human Receptors and Critical Groups

For risk-assessment purposes, the critical group for Chernobyl was selected to be individuals who were born in the year of the accident and who will live in the same contaminated location for 70 years (IAEA 1991 [156750], p. 207). Exposure of the population was from two main pathways: (1) the radiation dose to the thyroid as a result of the concentration of radioiodine and

similar radionuclides in the gland, and (2) the whole-body dose caused largely by external irradiation mainly from radiocesium (NEA 1995 [156632], p. 30). About 80% of the lifetime dose was accumulated in the first ten years after the accident (Los' and Poyarkov 2000 [157508], p. 194). A group of people that can be considered to include the reasonably maximally exposed individual includes pregnant women, fetuses, and school children (Lazjuk et al. 1995 [156626], p. 71). The risk of radiation for these people is correlated with the level of ^{137}Cs contamination, because ^{137}Cs is the most significant contributor to internal and external doses (see Section 13.3.9.2).

Doses received by the public are different for rural populations, including agricultural workers and "come-backers" living within the highly contaminated exclusion zone, and urban populations. Doses have varied with time since the Chernobyl accident.

13.3.9.2 Human Exposure Pathways

Exposure pathways to the populace resulting from the Chernobyl accident occurred through (1) external irradiation from radioactive materials deposited on the ground from the radionuclide fallout or accumulation from irrigation water, and (2) internal irradiation caused by inhalation of airborne materials and ingestion of contaminated foodstuff. Table 13.3-9 presents an example of the typical types of data for the city of Bragin, Belarus, and includes the following categories of data:

- Population (number of children and total inhabitants)
- Deposition density of ^{137}Cs and ^{90}Sr
- Exposure rate
- Concentration in foods
- Consumption rate of foods
- Internal dose.

This table also illustrates changes in the radionuclide concentration with time in different types of foods and actual internal doses in different population groups.

The dose received by the rural population makes up the bulk of the collective dose. Collective dose is the total dose over a population group exposed to a given source and is represented by the product of the average dose to the individuals in the group, multiplied by the number of persons comprising the group—for example, person-sievert (Sv) (NEA 1995 [156632], p. 59). Between 1986 and 1996, the rural population received 77% of the collective total effective dose. From 1986 to 1996, the mean annual collective effective internal dose was 65% versus 35% for the external dose for the rural areas (Los' and Poyarkov 2000 [157508], p. 186). In the urban areas, the main source of the internal dose was inhalation, while in the rural, agricultural areas, the internal dose consisted of both inhalation and ingestion of radionuclide particles.

About 95% of the contribution to external and internal doses to the rural population was by ^{137}Cs (Los' and Poyarkov 2000 [157508], p. 185). Based on Chernobyl investigations, the dose received by the public from TRU elements would be several dozen to several hundred times smaller than that from strontium and cesium over the 70-year period following the accident. Table 13.3-10a shows that the effective dose for the rural population is higher than that for the

urban population, because people in rural areas spent more time outdoors. The effective dose decreased rapidly for the first year after the accident, and then slowly until 1996. Table 13.3-10a presents changes in the effective dose of external radiation from ^{137}Cs with time. These values, if expressed in mrem/yr per pCi/m^2 (Table 13.3-10b), can be compared with BDCFs from external radiation for the Yucca Mountain Disruptive Event Scenario model. The annual value of 1 μSv/(kBq/m^2) corresponds to 3.7×10^{-6} mrem/yr per pCi/m^2.

Table 13.3-10c presents the BDCFs from the Yucca Mountain disruptive event scenario (CRWMS M&O 2001 [152536], Tables 11 and 13). Figure 13.3-12 shows that the calculated Yucca Mountain and observed Chernobyl BDCFs for ^{137}Cs are within the same order of magnitude for both minimum and maximum values. (To relate BDCF values using the method presented above to potential contamination at Yucca Mountain, the BDCF units reported in Table 5-17 of CRWMS M&O (2000 [151615]) have to be converted from mrem/yr per pCi/L to mrem/yr per pCi/m^2. Assuming that the wetted zone due to potential irrigation is 1 cm thick and the volumetric moisture content is 10%, 1 mrem/yr per pCi/L is equivalent to 1 mrem/yr per pCi/m^2.)

Table 13.3-11 shows maximum ^{137}Cs concentrations (kBq/m^2) in soils producing an internal radiation dose of 1 mSv/yr (100 mrem/year). The total radiation dose of 100 mrem/year is the annual permissible limit for the general public (DOE 1994 [104736], p. 2-6). The corresponding BDCFs for the internal radiation were calculated from the formula

$$\text{BDCF} = \text{Internal radiation dose} / \text{Radionuclide concentration activity of soil}$$

which is based on the BDCF definition given in CRWMS M&O (2000 [151615], Section 3.1.4.1). Because the Yucca Mountain model uses BDCFs in mrem/year per pCi/m^2, the concentrations in pCi/m^2 (Columns 4 and 5 of Table 13.3-11) were first calculated using the conversion factors 1 kBq = 27,027 pCi, and then the corresponding BDCFs (Columns 6 and 7 of Table 13.3-11) were calculated from the formula

$$\text{BDCFs} = 100 \text{ mrem/year} / \text{Concentration in soil (pCi/m}^2\text{)}$$

Because Table 13.3-11 presents maximum ^{137}Cs concentrations to obtain the annual dose of 1 mSv (1 mSv = 100 mrem), BDCFs calculated are minimal. These can be compared to BDCFs derived for both disruptive and nondisruptive contamination event pathways at Yucca Mountain as shown in Figure 13.3-13. For Chernobyl loamy soils, which have properties closer to Yucca Mountain soils than other types of soils, the BDCF is 1.25×10^{-5} mrem/yr per pCi/m^2 for tilled soils. This value is two to ten times higher than the minimal BDCFs for the Yucca Mountain disruptive contamination scenario. This difference occurs because contaminated groundwater is not taken into account when calculating BDCFs for the disruptive event scenario for Yucca Mountain (CRWMS M&O 2000 [151615], Section 3.3.2), while the use of contaminated groundwater contributed to the internal dose obtained after the Chernobyl accident. (Contaminated groundwater for the Yucca Mountain biosphere is included in dose calculations performed in the TSPA model once the radionuclide concentrations are estimated.) The critical group pathway analyses and sensitivity studies conducted for Yucca Mountain showed that the BDCF values for most radionuclides were dominated by only two consumption rates: water and leafy vegetables (CRWMS M&O 2000 [151615], Section 3.1.2.3). In contrast, Chernobyl data

showed that drinking groundwater was an insignificant contributor to the human dose (Bugai et al. 1996 [156596]). However, milk and milk products contributed significantly to the human dose (Table 13.3-12), more so than would be true for the Yucca Mountain critical population, because the consumption of milk products in Ukraine [the average is 0.18–1.5 L/day in different regions (Bar'yakhtar 1997 [156953], Table I.3.9–I.3.11)] is much higher than that in the United States. (The average used in the Yucca Mountain Biosphere Process Model is 0.011 L/day (CRWMS M&O 2000 [151615], Table 3-16)). More importantly, the short-lived radionuclides associated with the Chernobyl accident are far more significant contributors to human dose.

The IAEA (1991 [156750], Part E, pp. 222–237) estimated external and internal doses based on (1) direct measurements and (2) dose calculations in settlements located within the area with ^{137}Cs concentrations exceeding 550 kBq/m^2 (>15 Ci/km^2). Figures 13.3-13a indicates that a ^{137}Cs body concentration has a log-normal distribution across the population. Different dietary restrictions or habits (such as eating large quantities of forest mushrooms, an example relevant to Yucca Mountain in principle only) could cause variable body concentration distributions between different settlements. Figures 13.3-13b shows a significant scatter of data for the age-dependent distribution of ^{137}Cs.

Commercial fishermen on the Kiev reservoir, who consumed 360 kg/yr of fish in 1986, received 4.7×10^{-4} and 5×10^{-3} Sv from ^{90}Sr and ^{137}Cs, respectively (Berkovski et al. 1996 [156592], p. 41), i.e., the dose ratio of cesium to strontium was 10.6. The predicted contributions to the collective effective dose resulting from irrigation, municipal tap water, and fish for members of the general public for over 70 years following the ChNPP accident are shown in Table 13.3-13.

The predicted contribution of ^{90}Sr to the collective dose resulting from the use of Dnieper water is 80% (Berkovski et al. 1996 [156592], p. 42). Figure 13.3-14 presents the contribution of ^{90}Sr and ^{137}Cs in different components of food-chain pathways to averaged effective internal dose for Kiev in 1993. The contribution of radionuclides through the drinking-water pathway is different in different areas. For example, the drinking-water pathway contribution for the people of Kiev was about 6% of the total radiation dose; for the people of the southern Ukraine, it was 14% to 34% (Voitsekhovich et al. 1996 [156921], Figure 7).

Bugai et al. (1996 [156596]) estimated health risks caused by radionuclide migration to groundwater and compared these risks with risks from exposure to radioactive contamination on the ground surface. They determined that the estimated health risk to hypothetical, self-sufficient residents in the 30 km exclusion zone is dominated by external and internal irradiation from ^{137}Cs, caused mainly by ingestion of agricultural products. The estimated risk caused by drinking contaminated groundwater is approximately an order of magnitude lower. Strontium-90 migration via groundwater to surface water used in downriver population centers shows that groundwater can potentially only marginally contribute to the offsite radiological risk. Bugai et al. (1996 [156596], pp. 13–14) calculated the annual committed effective doses caused by consumption of ^{90}Sr-contaminated water, using an ingestion dose conversion factor of 3.9×10^{-5} mSv/Bq, determined by the Eckerman et al. (1988 [101069], Section II) formula. Committed effective dose equivalent is the resulting dose committed to the whole body from radionuclides absorbed internally over a 50-year period (DOE 1994 [104736], p. 2-3). Berkovski et al. (1996 [156592], p. 42) determined that consumption of drinking water in 1986 by the populace in the

Kiev region led to the maximum individual annual committed effective doses of 1.7×10^{-5} and 2.7×10^{-5} Sv from ^{90}Sr and ^{137}Cs, respectively.

13.3.9.3 Radiation Doses from Plutonium

An effective dose equivalent was used to assess the risk of inhalation of hot particles, accumulated on lungs from the Chernobyl accident, as a function of the distance between particles and α and β-radiation (Loshchilov et al. 1991 [156823], pp. 198, 202). The risk of lung cancer calculated based on the assumption of uniform distribution of radioactivity exceeds that calculated for a point source by a factor of two to three.

The most hazardous particles are those containing plutonium, which can contribute up to 40% of radioactivity in dust (Anokhova and Krivtsov 1991 [156829], p. 206). Calculations showed that the inhalation doses for agricultural laborers working on truck platforms are greater than external doses, and the Pu concentration exceeded the acceptable limit by an order of magnitude (Anokhova and Krivtsov 1991 [156829], pp. 209, 212). In the Yucca Mountain Biosphere Process Model for the disruptive event scenario, the sum of fractions of plutonium-238, -239, and -240 would exceed the contribution of other radionuclides (CRWMS M&O 2000 [151615], Table 3-23), as was observed at Chernobyl. Breathing air containing such high concentrations of plutonium for two months can lead to its accumulation in bones in concentrations exceeding the annual permissible limit (Anokhova and Krivtsov 1991 [156829], p. 209).

The main pathways for plutonium intake resulting from the Chernobyl accident are inhalation (which has been treated as an acute intake since 1986), uniform oral intake from food products, and inhalation of resuspended dust particles. Bondarenko et al. (2000 [156593], p. 475) calculated that the transfer factor of plutonium into grass is 0.3×10^{-3} (Bq/kg)/(Bq/m^2), and it could be as low as 0.15×10^{-6} (Bq/kg)/(Bq/m^2) due to the superficial contamination of grass. They also determined that the "soil-diet" transfer coefficient normalized to unit contamination density is 1.2×10^{-7} (Bq/kg)/(Bq/m^2). In this calculation, Bondarenko et al. (2000 [156593], p. 475), assumed that the "soil-diet" transfer coefficient is 2.4×10^{-5} (Bq/kg)/(Bq/m^2); the soil density is 2 g/cm^3; radioactivity is uniformly distributed within the top 10 cm soil profile; plutonium concentration in soils is 3,700 Bq/m^2, which is typical for the southeastern periphery of the exclusion zone; initial fallout particles of 1 μm in diameter, precipitating on inert soil particles, form agglomerates 5 μm in diameter; rural inhabitants spend one-third of the day outdoors; and the averaged resuspension coefficient is 10^{-9}/m.

Bondarenko et al. (2000 [156593], pp. 476–477) also presented data on the content of α-emitting isotopes of plutonium in the human skeleton. They found that the average plutonium content in 25 samples was 4.9×10^{-2} Bq for regions contaminated at the level of 20 mCi/km^2 (740 Bq/m^2). Table 13.3-14 presents the calculated content of α-emitting plutonium isotopes in the human skeleton in 1998 and compares these data with global fallout. This table indicates that the Chernobyl data exceeded that resulting from global fallout by 2.5–9.2 times.

13.4 SUMMARY AND CONCLUSIONS

Section 13.3 reviewed information from the Chernobyl accident regarding the exposure pathways, distribution of radioactive contaminants in the biosphere, and inputs to risk assessment

that may be relevant to future revisions of the Yucca Mountain Biosphere Process Model. Despite the difference in climatic conditions and the accident/potential-exposure scenarios for Chernobyl and Yucca Mountain, respectively, the Chernobyl data serve as a source of information to improve the confidence in a conceptual model of exposure pathways and process models. As part of the biosphere-model validation for both groundwater release and volcanic release scenarios, the YMP is interested in measurements that could represent input data in validating models for specific environmental processes, as listed in Section 13.2. The main conclusions that can be drawn from Chernobyl with respect to these processes and parameters are described below.

Radionuclide transfer from soil to plant via root uptake (see Section 13.3.8.2). Cesium migration from soils to grasses is relatively rapid. The radionuclide migration from roots into the tree trunks is limited by diffusion and advective radionuclide transfer from the soil (Bulgakov and Konoplev 2000 [156699]). Root uptake became a significant contributor to the food chain in the second year after the accident (Prister et al. 1991 [157548], p. 146).

Radionuclide transfer from soil to plants via atmospheric resuspension, including deposition of resuspended material on plant surfaces (see Section 13.3.5). Resuspension of radionuclides by wind-driven dust is an important factor after the tillage of agricultural lands, increasing the resuspension by more than an order of magnitude. Resuspended material is likely to settle on plant surfaces, thereby increasing their contamination. The Chernobyl data on hot-particle dispersal and dust transport showed that radionuclides attach to dust particles and move as combined particles. Aspects of models of atmospheric contaminant dispersal, radionuclide fallout, radionuclide resuspension, and particle-size distributions developed by Garger et al. (1999 [151483]), Goldman et al. (1987 [156820]), and Kashparov et al. (2000 [156622]) may be relevant to building confidence in a model for radionuclide resuspension resulting from a volcanic eruption through a potential Yucca Mountain repository.

Radionuclide transfer from animal food to animal products (see Sections 13.3.8.2 and 13.3.8.4). These data could be used in assessing the Yucca Mountain models for meat and milk contamination. Environmental half-life periods of decay of ^{137}Cs content in milk and agricultural products were shorter than those initially expected.

Removal of contaminants via erosion and leaching (see Sections 13.3.5 and 13.3.8.1). The average annual topsoil erosion in Ukraine from 1987 to 1990 contributed to the annual removal of 0.7×10^5 Bq/ha of ^{137}Cs from soils (Prister et al. 1991 [156824], Table 7). As a result of biochemical and physical-chemical processes, hot particles have been significantly dissolved by now, and radionuclides have been transferred to soils (Kashparov 2001 [156819], p. 37). The use of physical values of the half-life of radionuclides gives conservative estimates of radionuclide removal from soils in the Yucca Mountain Biosphere Process Model.

Inhalation of resuspended contamination material originally deposited on the ground (see Sections 13.3.5 and 13.3.9.3). The most hazardous particles associated with the Chernobyl accident are those containing plutonium, which can contribute up to 40% of radioactivity in the dust (Anokhova and Krivtsov 1991 [156829], p. 206). The inhalation doses for agricultural laborers are greater than the external doses, with the plutonium concentration exceeding the acceptable limit by an order of magnitude.

Radionuclide accumulation in soils and plants under irrigation using contaminated water (see Section 13.3.7). Irrigation using contaminated water creates radioactive contamination of both irrigated soils and agricultural products (Perepelyatnikov et al. 1991 [156822]; Bondar et al. 1991 [156846]). The increase in the concentration of radionuclides in soils during irrigation in the southern Ukraine, where environmental conditions are more similar to those at Yucca Mountain than are those in the Chernobyl vicinity, confirms the concept of a radionuclide-buildup factor used in the Yucca Mountain Biosphere Process Model.

In summary, results of the Chernobyl literature survey suggest that soil type influences the ecological half-life of radionuclides in the biosphere, both in regard to soil bioaccumulation factors and advective and diffusive transport properties that limit radionuclide transfer to plant roots. With respect to rural populations, agricultural methods—including irrigation and tillage—and crop types play an important role in resuspension of radionuclides. Resuspended material is likely to increase the contamination of plant surfaces. Resuspended radionuclides would increase the inhalation dose for agricultural workers, which would be particularly significant for plutonium associated with the Chernobyl accident.

Chernobyl data include both the relatively short-lived isotopes of iodine, cesium, and strontium, and long-lived transuranic elements such as plutonium and americium. Among the long-lived radionuclides of interest to Yucca Mountain, and not present at Chernobyl, are ^{129}I, ^{227}Ac, ^{232}U, ^{233}U, ^{237}Np, ^{243}Am, ^{210}Pb, ^{231}Pa, ^{226}Ra, ^{230}Th, and ^{242}Pu (CRWMS M&O 2000 [151615], Sections 3.3.1 and 3.3.2).

Numerous data collected for the past 15 years about the distribution and accumulation of radioactive materials in different parts of the biosphere after the Chernobyl accident, including the main exposure pathways and mechanisms of radioactive contamination of the environment and the population, can be used to build confidence in Yucca Mountain conceptual and numerical models. They can also be used to enhance models for long-term transport processes and radiation doses associated with possible exposure to radioactive material in the vicinity of the potential nuclear waste disposal site at Yucca Mountain. For the potential groundwater-contamination scenario at Yucca Mountain, radionuclide-contaminated water, which is to be used as the source of drinking water, irrigation, animal watering, and domestic uses, is expected to increase the likelihood of ingestion uptake of radionuclides by humans. Chernobyl data on the atmospheric distribution of contaminants, their fallout, and redistribution in soils and plants may be considered an anthropogenic analogue for the potential release of radionuclides caused by a volcanic eruption at Yucca Mountain, accompanied by atmospheric dispersal of contaminants into the environment through ash fallout on the land surface. Analogues related to volcanic processes are discussed in Section 14.

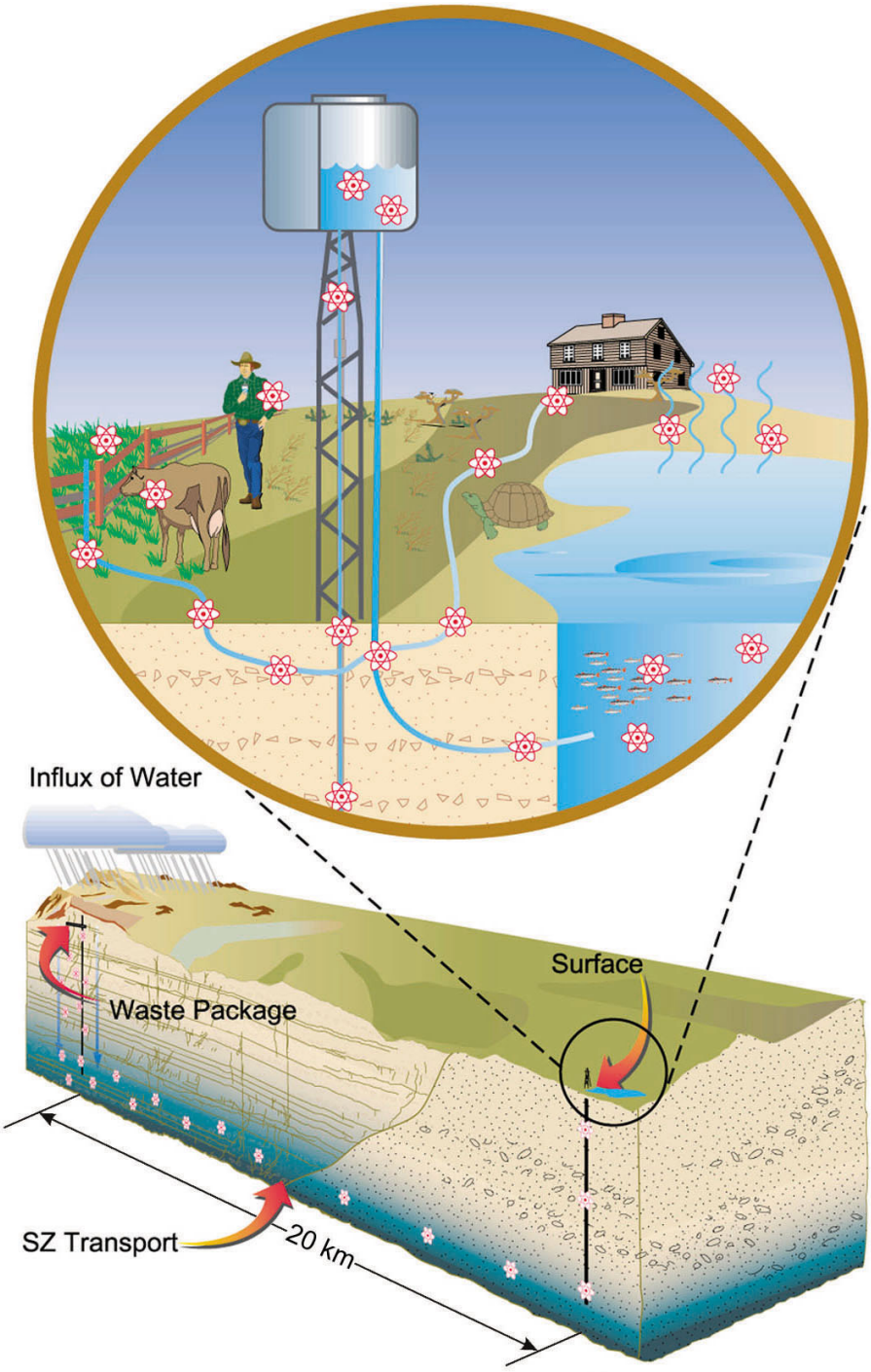

Source: CRWMS M&O 2000 [151615], Figure 3-1.

Figure 13.2-1. Illustration of the Biosphere in Relationship to the Potential Repository System

Source: Modified from Shestopalov 1996 [107844], p. 1.

Figure 13.3-1. Location of the ChNPP in (a) Europe, (b) Ukraine, and (c) the Kiev Region

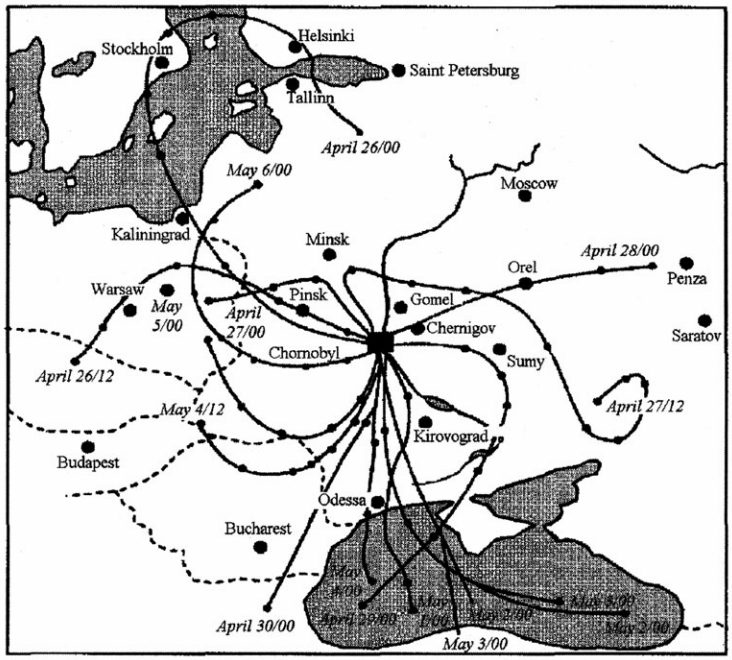

NOTE: Dashed lines indicate country boundaries, and Dates/Times indicate date and time (in hours) in 1986.

Source: Bar'yakhtar et al. 2000 [157504], Figure 2.5.2).

Figure 13.3-2. Fallout Trajectories of the ChNPP Accident

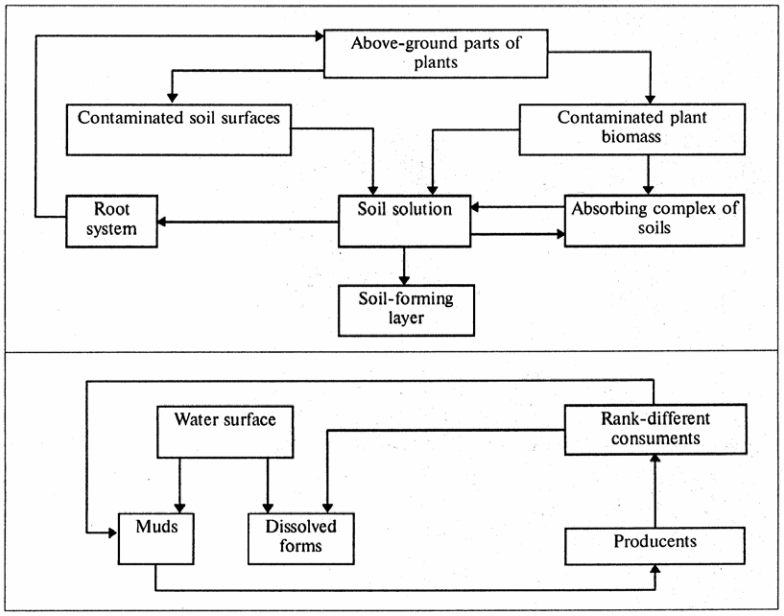

Source: Bar'yakhtar 1997 [156953], Figure I.3.19, p. 263.

Figure 13.3-3. Schematic Illustrating the Principal Pathways for the Radionuclides Entering the Biosphere through Terrestrial and Aquatic Ecosystems That Were Considered in Evaluating the Consequences of the Chernobyl Accident

a)

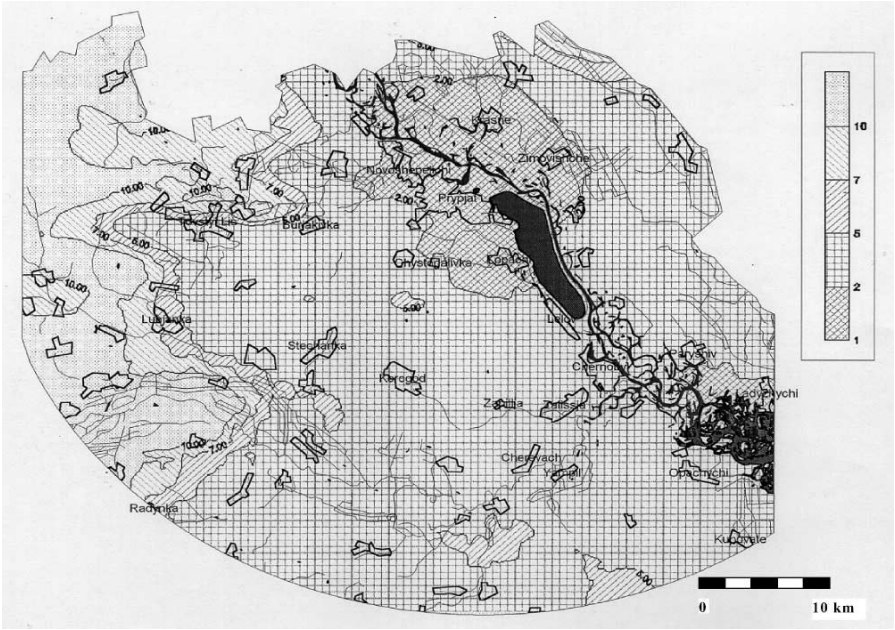

b)

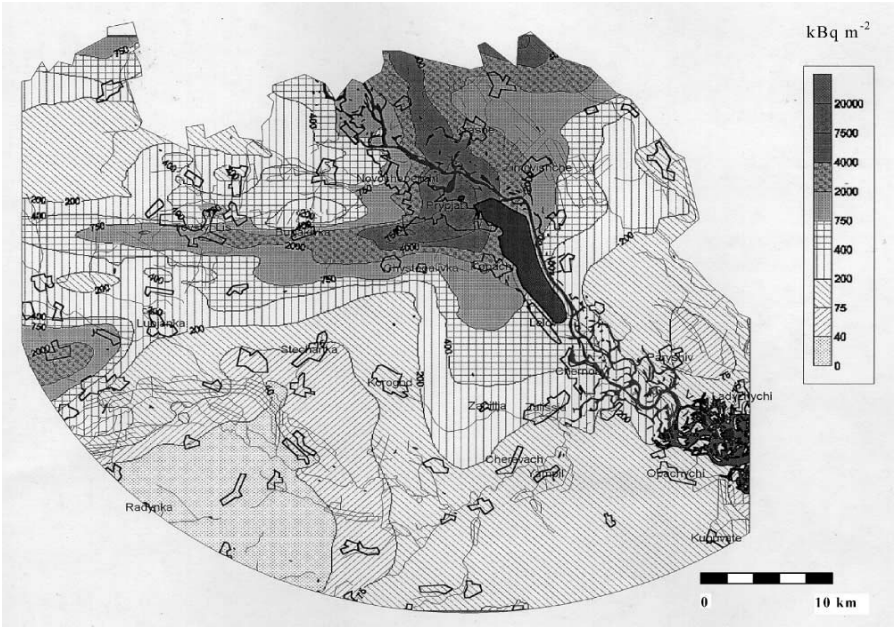

NOTE: Concentrations are kBq/m^2.

Source: Data of the Ukrainian Institute of Agricultural Radioecology (Kashparov et al. 2001 [157400], Figure 3, Figure 2).

Figure 13.3-4. Maps of the Terrestrial Contamination of the 30 km Chernobyl Exclusion Zone in Ukraine: (a) ^{90}Sr; (b) ^{137}Cs

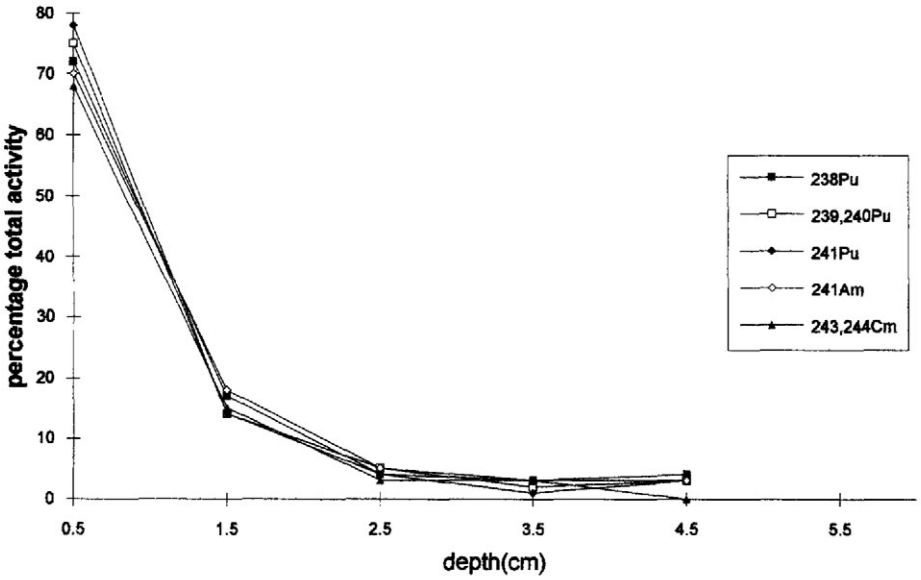

Source: Mboulou et al. 1998 [156628], Figure 1.

Figure 13.3-5. Vertical Distribution of Actinides in Soil to 4.5 cm

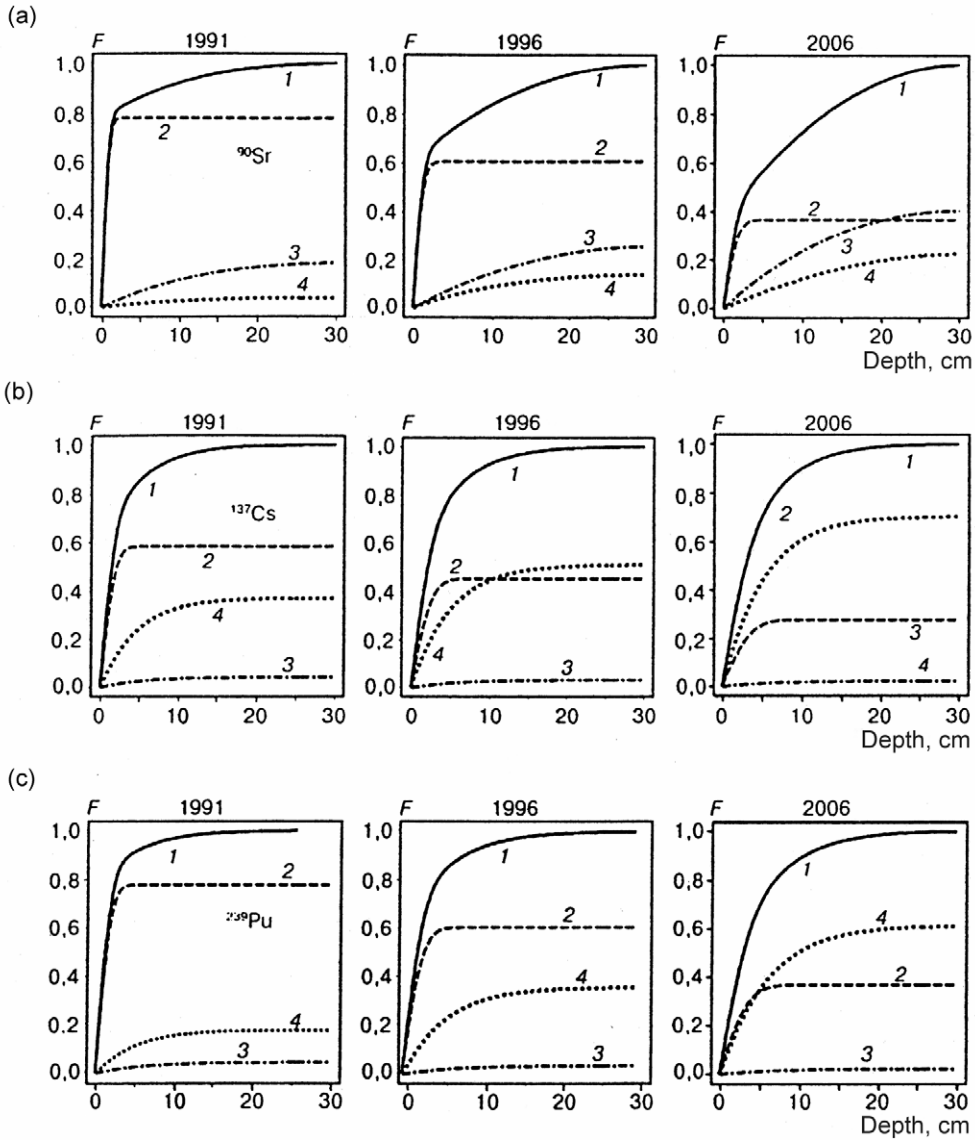

NOTE: 1 - total content, 2 - radionuclides in fuel particles, 3 - mobile forms, and 4 - absorbed forms.

Source: Ivanov 2001 [156818], p. 57.

Figure 13.3-6. Dynamics of Redistribution of ^{90}Sr (a), ^{137}Cs (b), and ^{239}Pu (c) as a Function of Depth and Time in Derno-podzolic Silt Soils

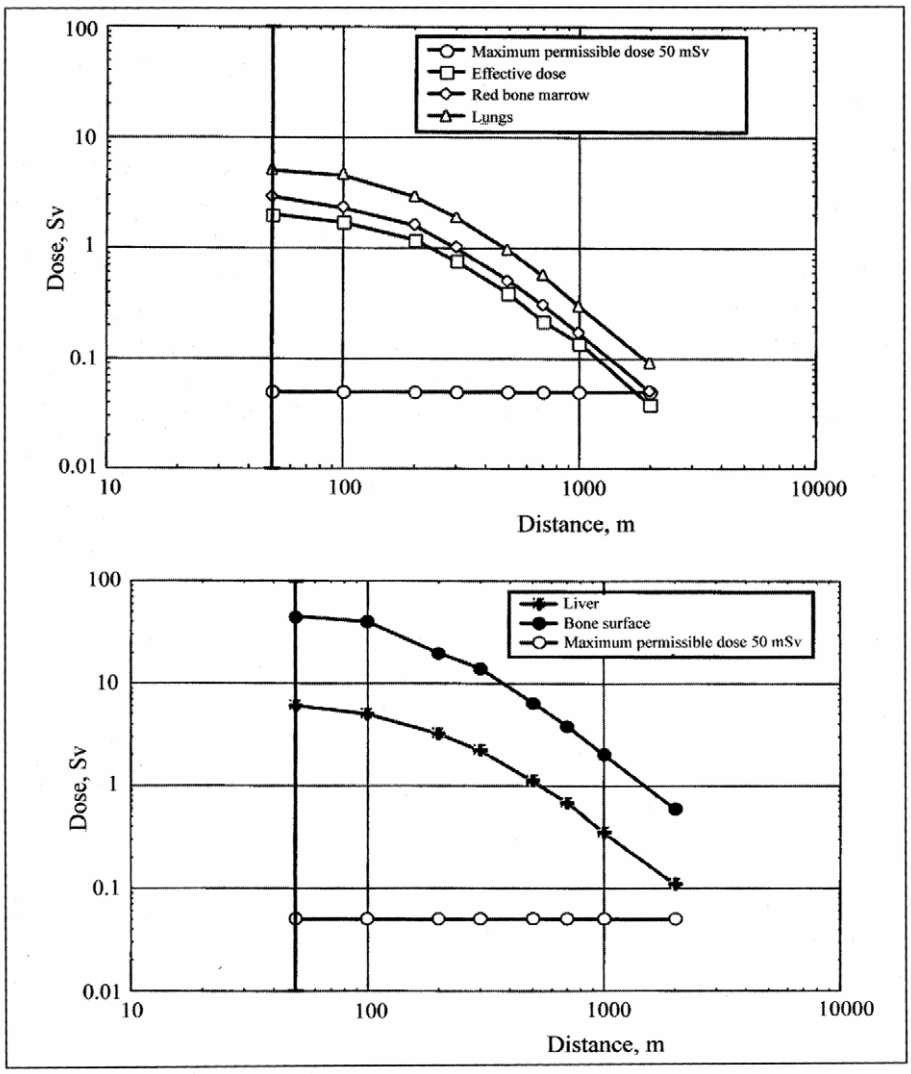

NOTE: For Pasquill weather Category C with no wind and speed of 4.2 m/s at 100 m altitude, which corresponds to a wind speed of 2.53 m/s at the surface.

Source: Bar'yakhtar et al. 2000 [157505], Figure 3.5.2.

Figure 13.3-7. Predicted Inhalation Doses as a Function of the Distance from the Hypothetical Collapsed Shelter

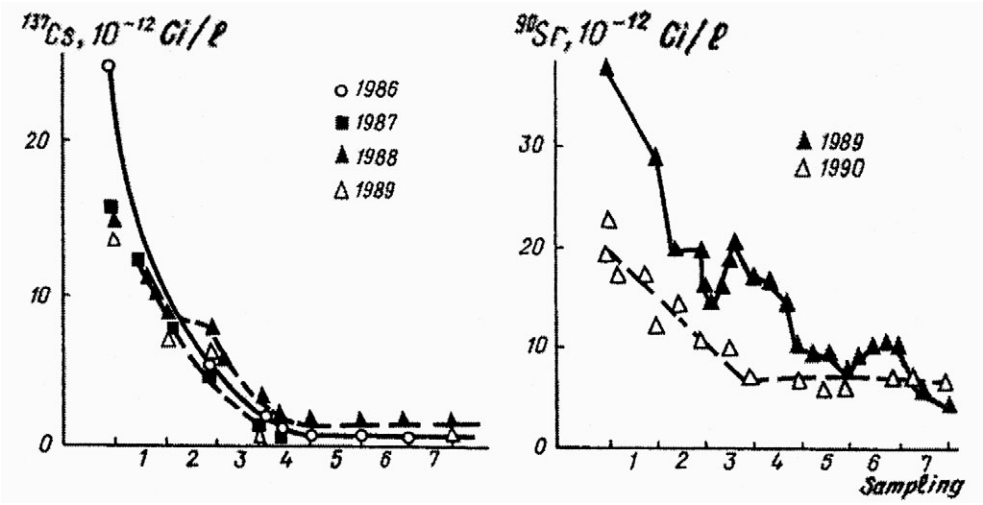

NOTE: 1: mouth of Pripyat; 2: Kiev Reservoir; 3: Kanev Reservoir; 4: Kremenchug Reservoir; 5: Dneprodzerzhinsk Reservoir; 6: Zaporozh'e Reservoir 7: Kakhovka Reservoir.

Source: Modified from Bar'yakhtar 1997 [156953], Figure I.3.16, p. 250.

Figure 13.3-8. Concentration of ^{90}Sr and ^{137}Cs in Water from Seven Sites along the Dnieper River

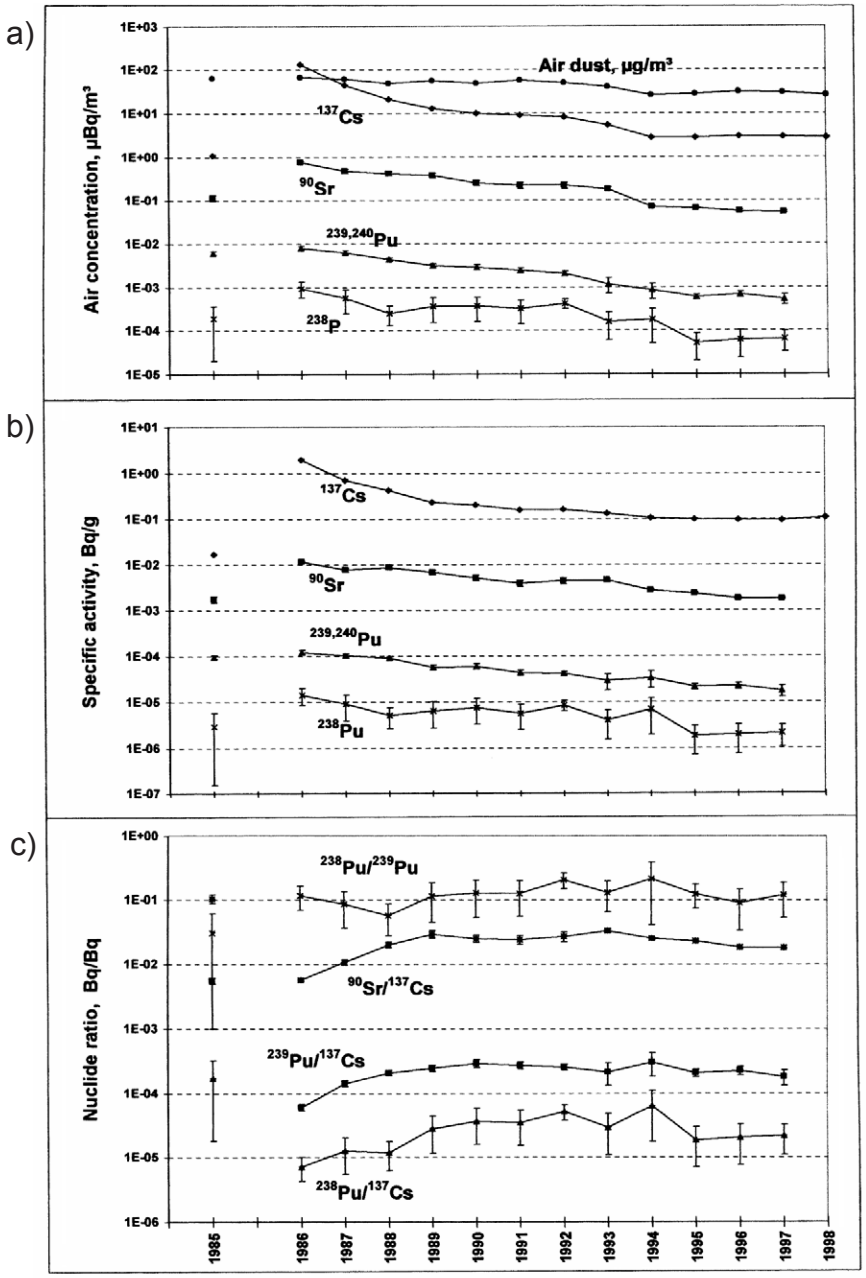

NOTE: All values are corrected for radioactive decay to 1 May 1986. Values for 1986 relate to the second half of the year only, i.e., the Chernobyl deposition phase is not included. The air-dust concentration ($\mu g/m^3$) is shown for comparison.

Source: Rosner and Winkler 2001 [156629], Figure 1.

Figure 13.3-9. Mean Values of (a) Radionuclide Concentrations in Air ($\mu Bq/m^3$), (b) Specific Activities in Air Dust (Bq/g), and (c) Radionuclide Ratios in Air (Bq/Bq) at Munich-Neuherberg Since 1985.

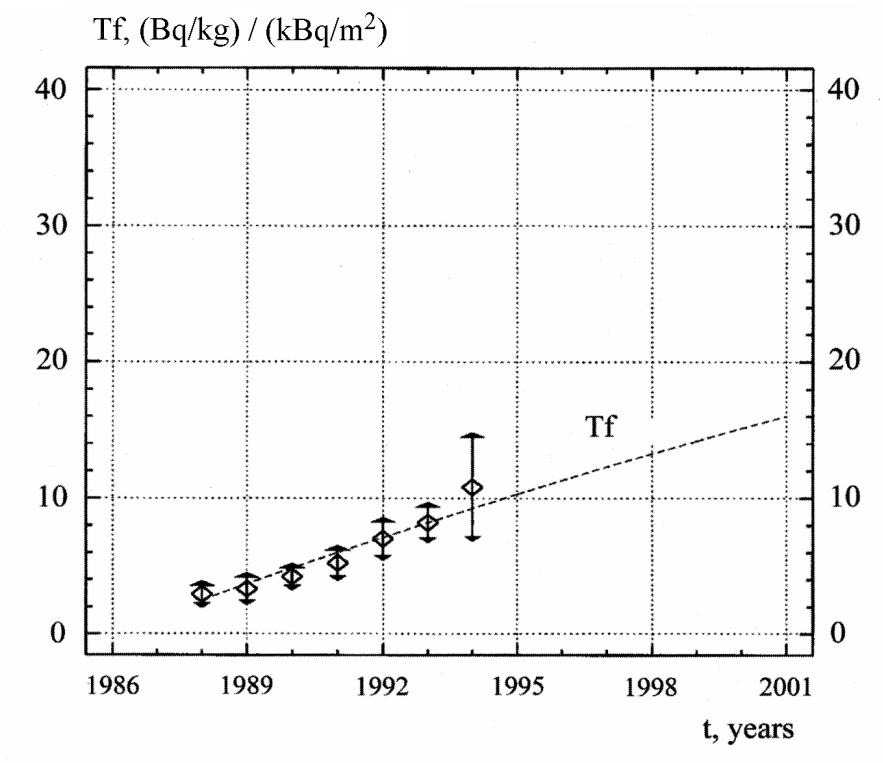

NOTE: Data points are experimental values; the line is the theoretical curve for pH=6.

Source: Bar'yakhtar et al. 2000 [157504], Figure 2-5.9.

Figure 13.3-10. Effective Meadow-Vegetation Transfer Coefficients for ^{90}Sr (T_f), Neglecting Redistribution in the Root Layer

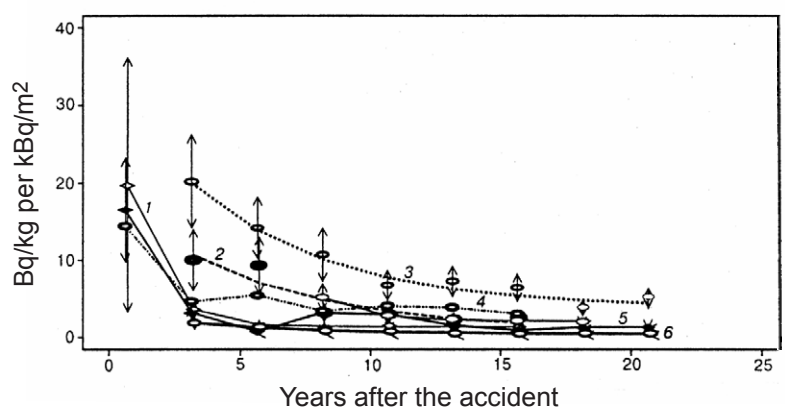

NOTE: 1, 2: derno-podzolic sandy soils; 3: derno-podzolic silty and sandy soils; 4: mineral soils with fuel traces; 5: derno-podzolic sandy soils with fuel traces; 6: loamy and clayey soils.

Source: Ivanov 2001 [156818], Figure 10, p. 63 (summarized the results of several authors).

Figure 13.3-11. Dynamics of the Soil-Plant Transfer Coefficient for ^{137}Cs, Which Is Approximated by a Function y = a exp(-bt) + (1-a) exp(-ct), for Meadow Grass Areas

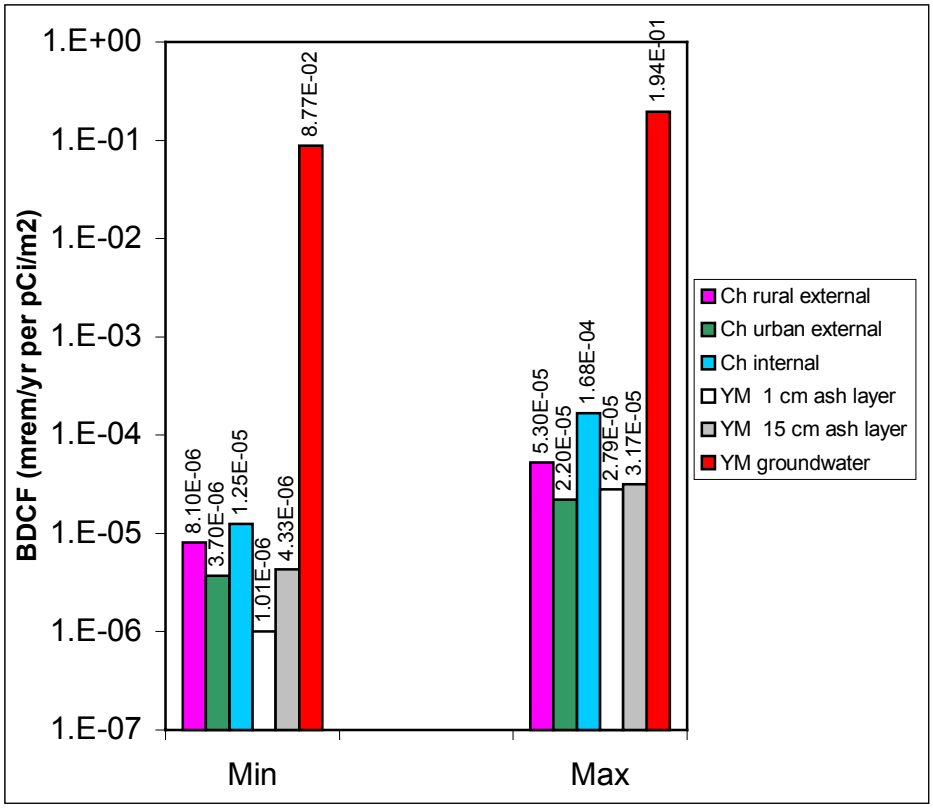

NOTE: For groundwater BDCF, refer to Section 13.3.9.2.

Chernobyl External Dose (Table 13.3-10b); Yucca Mountain (YM) Disruptive Event Contamination Scenario (Table 13.3-10c); and Internal Radiation for Soil Types for Chernobyl (Table 13.3-11).

Source: CRWMS M&O 2000, [151615], Table 3-17 (for Yucca Mountain Groundwater Contamination Scenario).

Figure 13.3-12. Comparison of Minimum and Maximum Values of ^{137}Cs BDCFs for Chernobyl (Ch) and Yucca Mountain

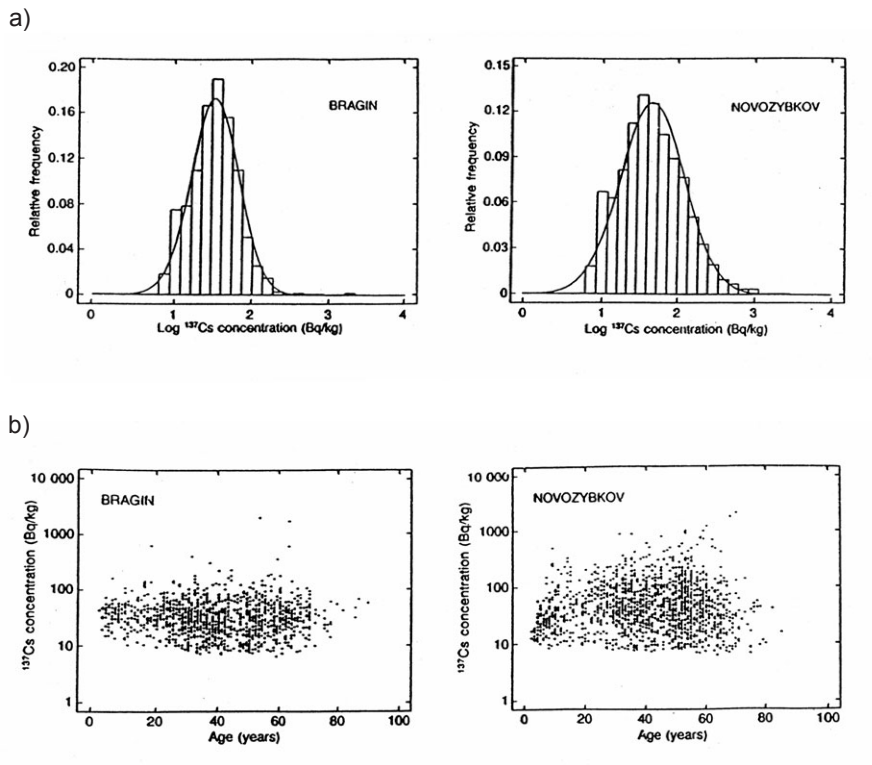

Source: (a) IAEA (International Atomic Energy Agency) 1991 [156750], p. 265;
(b) IAEA 1991 [156750], p. 263.

Figure 13.3-13. (a) Frequency Distributions of the Logarithm of ^{137}Cs Concentration in the Body at Two Selected Settlements (Bragin, Belarus, and Novozybkov, Russia); (b) Scatter Diagram of ^{137}Cs Concentration in the Body as a Function of Age

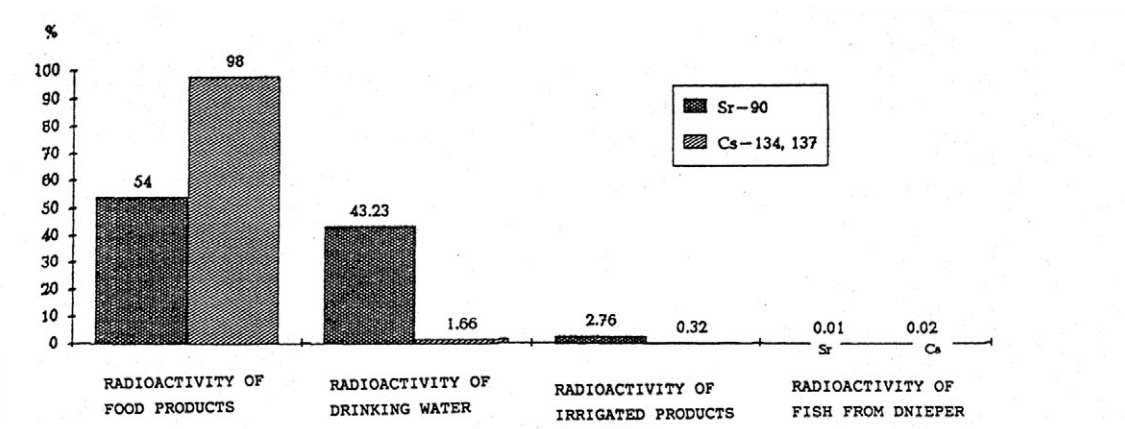

Source: Voitsekhovitch et al. 1996 [156921], Figure 8.

Figure 13.3-14. Contribution of ^{90}Sr and ^{137}Cs in Different Components of Food Chain Pathways to Averaged Effective Internal Dose for the Population of the City of Kiev (1993 scenario)

Table 13.3-1. Vertical Distribution of Plutonium and Uranium in Soils in the Vicinity of the ChNPP

Depth (cm)	$^{239(240)}$Pu (%)	Ratio ^{238}U/^{235}U
0-1	91-97	79.9-103.5
1-2	2.9-7.9	126.7-135.8
2-3	0.3-0.6	129.6-137.3
3-4	0-0.2	137.1-137.8
4-5	0-0.1	137.6-137.8

Source: Sobotovich 1992 [134218], Table 3.6.

Table 13.3-2. Typical Radioactive Contamination Levels (Bq/L) for Groundwater in the Inner Exclusion Zone

Source of water	^{90}Sr	^{137}Cs	$^{239+240}$Pu	^{241}Am
MPC (maximum permissible concentration)	14.8	555.5	81.5	70.3
Regional groundwater contamination	0.1-10	0.1-1	≤0.01	≤0.01
Shelter	10-10^3	0-100	--	--
Interim radioactive waste storage sites	10^2-10^4	0.1-10	≤0.01-1	≤0.01
Cooling pond	1-10^2	0.1-1	--	--
Artesian aquifer in Eocene deposits	≤0.01	≤0.01	--	--

Source: Shestopalov and Poyarkov 2000 [157507], Table 5.4.1.

Table 13.3-3. Percentages of Measured Concentrations of Radionuclides in Kiev Metropolitan Area Groundwater, 1992–1996

Aquifer	^{137}Cs Concentration, mBq/L				^{90}Sr Concentration, mBq/L		
	<10	10–50	51–150	>150	<10	10–50	>50
Quaternary	24%	56%	14%	6%	53%	40%	7%
Eocene	45%	41%	9%	5%	71%	21%	8%
Late Cretaceous (Cenomanian)–Early Jurassic (Callovian)	46%	31%	13%	10%	80%	20%	--
Middle Jurassic (Bajocian)	47%	28%	15%	10%	62%	35%	3%

NOTE: The depths tested are: Quaternary aquifer: 2–18 m; Eocene aquifer: 45–65 m; Late Cretaceous (Cenomanian)–Early Jurassic (Callovian) aquifer: 80–150 m; Middle Jurassic (Bajocian) aquifer: 200–300 m.

Source: Shestopalov and Poyarkov 2000 [157507], p. 150, Table 5.4.2.

Table 13.3-4. Cesium-137 Concentrations in Agricultural Products Grown on Lands Irrigated Using Water from the Dnieper River Reservoirs, Compared with Lands Irrigated by Water from Other Sources

Type of Plant	Year	Irrigation using Contaminated Water from Dnieper River Reservoirs (see Figure 13.3-8)				Irrigation Using Uncontaminated Water	
		Kanev	Kremenchuh	Dnepro-dzerzhinsk	Kakhovka	Kharkov Region	Donetsk Region
Winter wheat (seeds)	1987	50	50	25	30	8	10
	1988	30	40	10	30	10	10
Corn (seeds)	1987	10	10	5	6	2	2
	1988	10	5	6	3	1	2
Alfalfa	1987	600	600	370	320	80	100
	1988	400	400	300	200	90	90
Cabbage	1987	6	7	3	3	1	1
	1988	6	4	2	3	1	1
Tomato	1987	20	20	10	10	4	5
	1988	20	10	10	20	6	5
Tomato (vegetative mass)	1987	700	800	500	400	160	250
	1988	400	500	200	200	200	200
Cucumber	1987	40	40	20	20	10	10
	1988	30	40	20	10	10	20
Cucumber (vegetative mass)	1987	1,200	1,600	800	600	350	300
	1988	800	1,100	400	300	300	200

NOTE: ^{137}Cs reported as pCi/kg of air-dry mass

Source: Perepelyatnikov et al. 1991 [156822], p. 111, Table 5.

Table 13.3-5. Distribution of (a) ^{137}Cs and (b) ^{90}Sr in the Soil Profile beneath Rice Paddies in 1988 after Three Years of Irrigation, Southern Ukraine

a) ^{137}Cs (in pCi/kg of air-dry soil)

Soil layer (cm)	Year	Type of Agriculture					
	1986 1987 1988	Bare Bare Bare	Rice Alfalfa Fallow	Fallow Rice Alfalfa	Alfalfa Fallow Rice	Rice Fallow Rice	Rice Rice Rice
0–0.5		0.45	0.41	0.52	0.6	0.62	0.71
0.5–2		0.43	0.39	0.39	0.51	0.5	0.49
2–4		0.4	0.4	0.37	0.41	0.38	0.37
4–6		0.38	0.36	0.4	0.38	0.42	0.41
6–8		0.43	0.45	0.42	0.37	0.39	0.42
8–10		0.37	0.37	0.38	0.38	0.37	0.32
10–20		0.19	0.4	0.39	0.41	0.4	0.41
Average in a layer 0–20 cm		0.37	0.4	0.42	0.44	0.45	0.48
Contamination (Ci/km^2)		0.11	0.12	0.12	0.13	0.14	0.14

b) ^{90}Sr (in pCi/kg of air-dry soil)

Soil Layer (cm)	Year	Type of Agriculture					
	1986 1987 1988	Bare Bare Bare	Rice Alfalfa Fallow	Fallow Rice Alfalfa	Alfalfa Fallow Rice	Rice Fallow Rice	Rice Rice Rice
0–0.5		70	--	--	--	110	120
0.5–2		65	--	--	--	110	110
2–4		60	--	--	--	100	122
4–20		58	--	--	--	100	115
Average in a layer 0–20 cm		60	--	--	--	102	116
Contamination (Ci/km^2)		0.018	--	--	--	0.031	0.035

Source: Perepelyatnikov et al. 1991 [156822], pp. 109–110, Tables 2 and 3.

Table 13.3-6. Estimated Soil-to-Plant Transfer Factors for Yucca Mountain Compared with Those Determined from Observations After the Chernobyl Accident

Radionuclide	Soil-to-Plant Transfer Factors (Dimensionless)				
	Yucca Mountain				Chernobyl data
	Leafy	Root	Fruit	Grain	
Strontium	2.0E+00	1.2E+00	2.0E-01	2.0E-01	2.0E-02–1.2E+01
Yttrium	1.5E-02	6.0E-03	6.0E-03	6.0E-03	(3-70) x E-03
Cesium	1.3E-01	4.9E-02	2.2E-01	2.6E-02	2.0E-02–1.1E+00
Radium	8.0E-02	1.3E-02	6.1E-03	1.2E-03	(1-40) x E-03
Thorium	4.0E-03	3.0E-04	2.1E-04	3.4E-05	(1-700) x E-03
Uranium	8.5E-03	1.4E-02	4.0E-03	1.3E-03	1.6E-03–1.0E-01*
Neptunium	3.7E-02	1.7E-02	1.7E-02	2.7E-03	nE-02–nE-01**
Plutonium	3.9E-04	2.0E-04	1.9E-04	2.6E-05	nE-08–1.0E+00
Americium	2.0E-03	4.7E-04	4.1E-04	9.0E-05	nE-06–1.0E-01

NOTE: * Data are for ^{238}U; **n = any number from 1 to 10

Source: Bar'yakhtar 1997 [156953], p. 271 for Chernobyl; CRWMS M&O 2000 [151615], Table 3-10 for Yucca Mountain.

Table 13.3-7. Soil-to-Fodder Transfer Coefficients Determined after the Chernobyl Accident for ^{137}Cs

Crop	Soil Type and pH		
	Derno-podsol pH=4.5-5.5	Gray Forest pH=5.6-6.5	Chernozem pH=6.6-7.2
Hay from natural grass	10	4	1.8
Hay from planted grasses	4	3	1.6
Vetch	2.7	0.45	0.2
Clover	1.8	0.3	0.3
Lupine	1.5	0.4	0.15
Alfalfa	0.8	0.4	0.2
Silage	0.4	0.2	0.08
Fodder beet	0.5	0.35	0.2
Potato	0.25	0.13	0.045
Winter grain	0.5	0.2	0.05
Rye	0.4	0.1	0.04
Barley	0.3	0.1	0.06

NOTE: ^{137}Cs reported as (Bq/kg) / (kBq/m^2) (mean for 1987–1990).

Source: Shestopalov and Poyarkov 2000 [157507], p. 174, Table 5.6.2

Table 13.3-8. Concentrations of ^{137}Cs in Pasture, Meat and Milk, and Calculated Transfer Coefficients

Pasture Contamination (Bq/kg)	Intake* (kBq/day)	Meat (Bq/kg)	Milk (Bq/kg)	Transfer coefficients	
				Meat (day/kg)	Milk (day/L)
250	17.5	280	112	1.6E-02	6.4E-03
500	36	700	280	1.9E-02	7.8E-03
1,000	70	1,400	550	2.0E-02	7.9E-03
1,500	105	2,100	840	2.0E-02	8.0E-03
2,000	140	2,800	1,120	2.0E-02	8.0E-03
3,000	210	4,200	1,680	2.0E-02	8.0E-03
5,000	350	7,000	2,800	2.0E-02	8.0E-03
10,000	700	14,000	5,600	2.0E-02	8.0E-03

NOTE: *Assumes daily intake of 70 kg fresh herbage/animal. For comparison, in the Yucca Mountain biosphere model, the dairy and beef cow feed consumption rates are 55 and 68 kg/day, respectively (CRWMS M&O [151615], Table 3-13).

Source: Richards and Hance 1996 [157613]. Only equilibrium concentrations are included in the table.

Table 13.3-9. Example of the Database to Assess Radiation Dose for the City of Bragin, Belarus

Population					
Population Group	**1986**	**1987**	**1988**	**1989**	**1990**
Children	1,667	--	--	2,065	--
Total inhabitants	5,600	4,900	--	5,888	--
Deposition Density (kBq/m^2)					
Radionuclide	**1986**	**1987**	**1988**	**1989**	**1990**
Cesium-137	1,700	1,000	270 (5–1,000) [1)] (n = 8) [2)]	1,000 (n = 18) 830 (n = 50)	--
Strontium-90	--	--	--	78 (n = 9)	--
Exposure Rate (μR/h)					
	1986	**1987**	**1988**	**1989**	**1990**
Measurement	8,000 (10 May)	680 (10 May)	--	--	--
Concentration in Foods (Bq/kg) (approximate median values) (Data from Institute of Agricultural Radiology, Gomel)					
	1986	**1987**	**1988**	**1989**	**1990**
Milk	1,600	1,500	220	300	260
Root vegetables	740	630	330	370	370
Green vegetables	3,700	740	370	300	220
Vegetables/fruit	1,100	590	300	220	330
Berries, mushrooms	2,200	1,100	1,300	2,600	1,100
Honey	1,300	1,900	1,500	300	300
Eggs	1,300	190	190	190	300
Meat	1,700	1,100	740	260	300
Fish	--	1,800	740	1,500	220

Consumption Rate (g/day)		
Food Item	**Rural settlement**	**All Belarus**
Milk	735	690–710
Bread, white	220	240
Bread, dark	350	350
Potatoes	540	680
Vegetables	190	240
Fruit, berries	160	150
Berries	--	1.5
Mushrooms	6	7
Meat	150	180
Fish	46	60

Internal Dose (mSv) (Data for 1986, 1987: Institute of Biophysics, Moscow; data for 1988, 1989: Institute of Radiation Medicine, Minsk)						
$^{134+137}$Cs		**1986**	**1987**	**1988**	**1989**	**1990**
Average	Children Teenagers Adults	2 (n = 292) 5 (n = 87) 4 (n = 683)	1 (n = 94) 3 (n = 131) 3 (n = 111)	0.2 (n = 203) 0.2 (n = 731) 0.3 (n = 641)	0.1 (n = 3) 0.1 (n = 3) 0.2 (n = 131)	-- -- --
Maximum	Children Teenagers Adults	15 22 12	7 17 8	-- -- --	-- -- --	-- -- --
90th percentile	Children Teenagers Adults	10 13 8	5 7 5	-- -- --	-- -- --	-- -- --

NOTE: [1)] Range
[2)] Number of measurements

Source: IAEA 1991 [156750], Part E, Table 2-1.

Table 13.3-10a. Dynamics of the Effective Dose of External Radiation to Ukrainians from ^{137}Cs Contamination after the Chernobyl Accident

Population group	Year										
	1986*	**1987**	**1988**	**1989**	**1990**	**1991**	**1992**	**1993**	**1994**	**1995**	**1996**
Urban	6.0	1.5	1.4	1.4	1.3	1.3	1.2	1.2	1.1	1.0	1.0
Rural	14.3	3.5	3.4	3.3	3.2	3.1	3.0	2.7	2.5	2.4	2.2

NOTE:* 1986 data were estimated after the accident. ^{137}Cs reported for 1986–1996, $\mu Sv/(kBq/m^2)$

Source: Los' and Poyarkov 2000 [157508], Table 6.2.1, p. 187.

Table 13.3-10b. Calculated BDCFs for ^{137}Cs after the Chernobyl Accident

Population group	Year										
	1986	**1987**	**1988**	**1989**	**1990**	**1991**	**1992**	**1993**	**1994**	**1995**	**1996**
Urban	2.2E-05	5.6E-06	5.2E-06	5.2E-06	4.8E-06	4.8E-06	4.4E-06	4.4E-06	4.1E-06	3.7E-06	3.7E-06
Rural	5.3E-05	1.3E-05	1.3E-05	1.2E-05	1.2E-05	1.1E-05	1.1E-05	1.0E-05	9.3E-06	8.9E-06	8.1E-06

NOTE: See Section 13.3.9.2. Units in mrem/yr per pCi/m^2

Source: Table 13.3-10a.

Table 13.3-10c. Yucca Mountain BDCFs for ^{137}Cs for the Disruptive Event Scenario for the Transition Phase, 1 cm and 15 cm Ash Layers and Annual Average Mass Loading

	1–cm ash layer	**15–cm ash layer**
BDCFs	**mrem/yr per pCi/m^2**	**mrem/yr per pCi/m^2**
Mean	1.86E-06	5.81E-06
Min	1.01E-06	4.33E-06
Max	2.79E-05	3.17E-05

Source: Modified from CRWMS M&O 2001 [152536], Tables 11 and 13.

Table 13.3-11. Maximum ^{137}Cs Concentrations in Soils Producing Internal Dose of 1 mSv/yr and Calculated BDCFs

1	2	3	4	5	6	7
Soil Type	**Concentration kBq/m^2**		**Concentration pCi/m^2**		**BDCF mrem/yr per pCi/m^2**	
	Meadow	**Tilled**	**Meadow**	**Tilled**	**Meadow**	**Tilled**
Peat-bog	22	93	594,594	2,513,511	1.68E-04	3.98E-05
Sandy podzolic	74	130	1,999,998	3,513,510	5.00E-05	2.85E-05
Light-gray podzolic	148	185	3,999,996	4,999,995	2.50E-05	2.00E-05
Loamy chernozem	222	295	5,999,994	7,972,965	1.67E-05	1.25E-05

Source: Shestopalov and Poyarkov 2000 [157507], Table 5.6.4.

Table 13.3-12. Comparison of the Pathway Contribution (%) of Radionuclides Determined from Observations after the Chernobyl Accident in 1993

	^{90}Sr			**^{137}Cs**		
	Meat	**Leafy vegetables**	**Milk and milk products**	**Meat**	**Leafy vegetables**	**Milk and milk products**
Yucca Mountain	5 (10)	34 (42)	0 (2)	12 (4)	16 (3)	2 (0)
Chernobyl	4	19	54	8	2	74

Source: Yucca Mountain—CRWMS M&O 2000 [151615], Table 3-21; CRWMS M&O 2000 [151615], Table 3-24 (in parentheses)
Chernobyl— Berkovski et al. 1996 [156592], p. 41.

Table 13.3-13. Relative Contributions to the Collective Effective Dose from ^{137}Cs and ^{90}Sr, Resulting from the Chernobyl Accident

Region/Source (%)	Irrigation	Municipal Tap Water	Fish
Kiev Region	18	43	39
Poltava Region	8	25	67
Crimean Republic *	50	50	0

NOTE: * No Dnieper River fish consumed in Crimean Republic

Source: Berkovski et al. 1996 [156592], p. 42.

Table 13.3-14. Calculated Content (Bq) of α-emitting Pu Isotopes in the Human Skeleton in 1998 for the Ukraine-Belarus Territory with Contamination Density of 20 mCi/km^2 (740 Bq/m^2) and Comparison of These Data with Global Fallout

Type of Intake	From Global Fallout	From Chernobyl Fallout
Primary inhalation	1.3×10^{-3}	1.2×10^{-2}
Peroral due to superficial contamination	1.6×10^{-3}	0.56×10^{-2}
Peroral, biologically accessible forms	3.2×10^{-5}	1.1×10^{-4}
Inhalation due to resuspension	1.42×10^{-6}	3.6×10^{-6}
Total	2.9×10^{-3}	1.8×10^{-2}

Source: Bondarenko et al. 2000 [156593], Table 2.